BULLETIN N° 238
ACADÉMIE EUROPÉENNE
INTERDISCIPLINAIRE
DES SCIENCES

INTERDISCIPLINARY EUROPEAN ACADEMY OF SCIENCES

Lundi 7 octobre à 16h30
à l'Institut Curie, Amphi BURG salle annexe 2
12, rue Lhomond 75005 PARIS

Conférence :
"Organisation spatiale et temporelle à l'échelle mésoscopique
d'une protéine de signalisation cellulaire "
par Mathieu COPPEY Directeur de Recherche CNRS

Chef d'équipe Imagerie et contrôle de l'organisation cellulaire (LOCCO)
UMR168 – Laboratoire Physico-Chimie Curie
INSTITUT CURIE 20 rue d'Ulm, 75248 Paris Cedex 05

Notre Prochaine séance aura lieu le lundi 4 novembre 2019 à 17h
à l'Institut Curie, Amphi BURG salle annexe 2
12, rue Lhomond 75005 PARIS
Métros: Maubert Mutualité/Cardinal Lemoine (ligne 10)

Elle aura pour thème

ASSEMBLEE GÉNÉRALE ANNUELLE de l'AEIS

ACADÉMIE EUROPÉENNE INTERDISCIPLINAIRE DES SCIENCES
INTERDISCIPLINARY EUROPEAN ACADEMY OF SCIENCES

PRÉSIDENT : Pr Victor MASTRANGELO
VICE PRÉSIDENT : Pr Jean-Pierre FRANÇOISE
VICE PRÉSIDENT BELGIQUE(Liège):
Pr Jean SCHMETS
VICE PRÉSIDENT ITALIE(Rome):
 Pr Ernesto DI MAURO
SECRÉTAIRE GÉNÉRALE : Irène HERPE-LITWIN
TRÉSORIÈRE GÉNÉRALE: Édith PERRIER

MEMBRE S CONSULTATIFS DU CA :
Gilbert BELAUBRE
François BÉGON
Bruno BLONDEL
Michel GONDRAN

PRÉSIDENT FONDATEUR : Dr. Lucien LÉVY (†)
PRÉSIDENT D'HONNEUR : Gilbert BELAUBRE

CONSEILLERS SCIENTIFIQUES :
SCIENCES DE LA MATIÈRE : Pr. Gilles COHEN-TANNOUDJI
SCIENCES DE LA VIE ET BIOTECHNIQUES : Pr Ernesto DI MAURO

CONSEILLERS SPÉCIAUX:
ÉDITION: Pr Robert FRANCK
RELATIONS EUROPÉENNES :Pr Jean SCHMETS
RELATIONS avec AX: Gilbert BELAUBRE
RELATIONS VILLE DE PARIS et IDF:
Michel GONDRAN et Claude MAURY
MOYENS MULTIMÉDIA et UNIVERSITÉS: Pr Alain CORDIER
RECRUTEMENTS: Pr. Sylvie DERENNE
SYNTHÈSES SCIENTIFIQUES: Jean-Pierre TREUIL
MECENAT: Pr Jean Félix DURASTANTI
**GRANDS ORGANISMES DE RECHERCHE NATIONAUX ET
INTERNATIONAUX:** Pr Michel SPIRO
THÈMES ET PROGRAMMES DE COLLOQUES: Pr Jean SCHMETS

SECTION DE NANCY :
PRESIDENT : Pr Pierre NABET

octobre 2019

N°238

TABLE DES MATIERES

Prochaine séance : lundi 4 novembre 2019

ASSEMBLEE GÉNÉRALE ANNUELLE de l'AEIS

ACADEMIE EUROPEENNE INTERDISCIPLINAIRE DES SCIENCES
Fondation de la Maison des Sciences de l'Homme, Paris.

Séance du Lundi 7 octobre 2019/IHP 16h30

La séance est ouverte à 16h30 **sous la Présidence de Victor MASTRANGELO** et en la présence de nos Collègues Gilbert BELAUBRE, Jean BERBINAU, Eric CHENIN, Gilles COHEN-TANNOUDJI, Françoise DUTHEIL, Michel GONDRAN, Jean -Pierre FRANCOISE, Irène HERPE-LITWIN, Claude MAURY, Edith PERRIER, Jacques PRINTZ, Jean SCHMETS, Michel SPIRO, Jean-Pierre TREUIL, Jean-Paul TEYSSANDIER.

.

Etait également présent notre collègue, membre correspondant Benoît PRIEUR.

Etaient excusés :François BEGON, Jean BERBINAU, Jean-Pierre BESSIS, Bruno BLONDEL, Jean-Louis BOBIN, Michel CABANAC, Alain CARDON, Juan-Carlos CHACHQUES, Alain CORDIER , Daniel COURGEAU, Sylvie DERENNE, Ernesto DI MAURO, Jean-Félix DURASTANTI, Claude ELBAZ, Vincent FLEURY, Robert FRANCK, Dominique LAMBERT, Pierre MARCHAIS, Anastassios METAXAS, Jacques NIO, Marie-Françoise PASSINI, Pierre PESQUIES, Denise PUMAIN, René PUMAIN, Alain STAHL,

I. Conférence de Mathieu COPPEY

A. Présentation du conférencier par notre Président Victor MASTRANGELO

– **Position actuelle**

Depuis Aout 2018, directeur de l'équipe LOCCO « light-based observation and control of cell organization » *suite au décès prématuré de Maxime Dahan survenu en juillet 2018*. Unité UMR168, département de physico-chimie Institut Curie, Paris. Affilié UMPC, PSL*, EDPIF, IPGG.

Depuis septembre 2019, directeur adjoint de l'UMR168, aux côtés de Pascal Hersen.

– **Domaines d'intérêts**

- Biophysique, biologie cellulaire, biologie du développement.
- Microscopie optique, optogénétique, suivi de molécule unique.
- Physique statistique, processus stochastiques, réaction-diffusion, auto-organisation.
- Modélisation, analyse d'image, biologie quantitative.

– **Parcours de recherche**

2019 : HDR et Directeur de Recherche DR2 CNRS.
2013-2018 : Chercheur CNRS CR1 dans l'équipe LOCCO de Maxime Dahan à L'institut Curie, PCC.
2010-2013 : Chercheur CNRS CR1 dans l'équipe « Optique et Biologie » de Maxime Dahan à l'IBENS-LKB, Ecole Normale Supérieure de Paris. Recruté CR1 dans la commission interdisciplinaire 54 (2010) et titularisé commission 05 (2011).
2008-2010 : Postdoctorat dans l'équipe « Optique et Biologie » de Maxime Dahan à l'IBENS-LKB, Ecole Normale Supérieure de Paris. *Sujet : Contrôle magnétique de la polarité.*

2005-2008 : Postdoctorat dans l'équipe de Stanislav Shvartsman, Lewis-Sigler Institute for Integrative Genomics, Princeton University. *Sujet : Gradients morphogénétiques de l'embryon précoce de Drosophile.*
2004-2005 : séjour postdoctoral chez Jean-Pierre Rospars, Institut National de la Recherche Agronomique, Versailles, France. *Sujet : Cascade de la protéine G dans les neurones récepteurs olfactifs.*

- **Education**

2002-2004 : Thèse de physique statistique sous la direction du Prof. Michel Moreau au Laboratoire de Physique Théorique de la Matière Condensée LPTMC, Université Paris VI UPMC, Paris, France. *Sujet : Etude stochastique des réactions limitées par le transport.* Bourse ministérielle et monitorat à l'UMPC
2003-2004 : Master2 en auditeur libre, « Approche Interdisciplinaire du vivant » AIV, CRI, Necker, Paris.
2001-2002 : Master2 « Modélisation dynamique et statistique des systèmes complexe », UMPC Paris.
1996-2001 : Licence et Master parcourt « science de la matière » UMPC Paris.
1996 : Baccalauréat scientifique.

- **Enseignements**

2011-2018 : UE Licence 3 « modélisation en biologie », Ecole Normale Supérieure, Paris.
2011-2018 : Interventions diverses Master 2 et cours doctoraux, ENS, Curie, UPMC. **2010-2013 : UE Master 1** « biologie des systèmes », Centre de recherche interdisciplinaire CRI – AIV.
2002-2004 : Monitorat en DEUG science de la matière, UPMC Paris. 60hrs/an.

- **Publication et métrique**

46 publications, h-index 22 (Google Scholar)

- **Animation scientifique**

Il a réalisé de nombreuses animations scientifiques parmi lesquelles :

- **2012 : Atelier INSERM 217 « Photocontrôle et optogénétique des systèmes et fonctions biologiques »**:
- **2010- 2013 : Séminaire Hebdomadaire de biophysique de l'ENS.**
- **2014, 2015, 2016: Organisateur local du « Circle Meeting »**. Conférence de deux jours destinée à ~80 postdoctorants et doctorants venant de 6 grandes structures de recherche européennes (Amsterdam, Londres, Saarbrücken, Dresden, Heidelberg, et Paris).
- **2014, 2016, et 2018 : Co-organisateur du cours Curie international** « Multiscale integration in biological systems ». Les cours sont accessibles sur : https://www.youtube.com/playlist?list=PLe9eFu6aHpLxEIFGFri9o6QQGKL1eQZIB

- **2016: Co-organisation du French Opto Club**. Conférence d'une journée avec ~100 participants sur l'optogénétique.
- **2017 : Organisation des journées annuelles du GDR3070 « CellTiss »** à Mandres les Roses. Conférence de 3 jours avec 100 participants sur les thèmes de la biophysique. Les informations sur ce GDR peuvent être consultées en ligne : http://nonlineaire.univ-lille1.fr/GDR3070/

Il a par ailleurs été **rapporteur** pour plusieurs revues internationales telles que Journal of Chemical Physics, Biophysical journal, Biochemistry, Chaos, Trends in Biotechnology, PNAS, Plos one, Nature Communication, membre du jury de 4 thèses et tuteur de 4 étudiants et encadré les travaux de nombreux post-doctorants.

B. **Conférence**

Résumé de la conférence:

Organisation spatiale et temporelle à l'échelle mésoscopique d'une protéine de signalisation cellulaire

par Mathieu COPPEY Directeur de Recherche CNRS
Chef d'équipe Imagerie et contrôle de l'organisation cellulaire (LOCCO)
UMR168 – Laboratoire Physico-Chimie Curie
INSTITUT CURIE 20 rue d'Ulm, 75248 Paris Cedex 05

La description et la compréhension des états de la matière à l'échelle mésoscopique dans les systèmes biologiques représentent un des grands enjeux de la biophysique actuelle pour deux principales raisons. Du point de vue fondamental, cette échelle est celle de la transition entre le chaos moléculaire -les molécules soumises à l'agitation thermique effectuent des processus aléatoires- et les premières structures organisées – les molécules forment des assemblages robustes dont la fonction est déterministe-. Du point technique, cette échelle est longtemps restée inaccessible à l'observation, la microscopie optique étant intrinsèquement limitée à une résolution de l'ordre de 200 nanomètres. Après avoir introduit l'échelle mésoscopique en biologie cellulaire, j'illustrerai cet enjeu en présentant nos résultats obtenus sur une protéine de signalisation, la protéine Rac1. La signalisation cellulaire consiste en des cascades de réactions biochimiques qui permettent à la cellule de se réguler, de sentir son environnement et d'agir en conséquence. En utilisant des techniques de molécule unique pour la microscopie de super-résolution et des techniques d'optogénétique, nous avons pu montrer que la protéine Rac1 forme des agrégats nanoscopique de composition hétérogène. La distribution asymétrique de ces agrégats en gradients subcellulaire contrôle les processus cellulaires tels que la migration. Le concept qui émerge de ces résultats ainsi que ceux de la communauté, est que les objets moléculaires en biologie s'organisent et interagissent collectivement. L'idée d'interaction stéréospécifique, ou plus communément « clef-serrure » doit être étendue à une nouvelle physique qui intègrent les effets collectifs reposant sur des interactions multivalentes de basses affinités.

Un compte-rendu rédigé par un membre de l'AEIS sera prochainement disponible sur le site de l'AEIS http://www.science-inter.com.

Annonces

I. Le Président Victor MASTRANGELO et le Bureau de l'AEIS ont la grande douleur de vous annoncer le décès de notre Collègue Jean-Paul TEYSSANDIER survenu très brusquement le 16 octobre 2019.

Ancien élève de l'Ecole Polytechnique , Ingénieur des Ponts et Chaussées, ancien Professeur au CNAM, membre de l'Académie des Technologies, il s'était principalement distingué dans les Etudes de structures innovantes, en particulier dans le domaine des ponts. Il s'intéressait par ailleurs beaucoup à l'astrophysique. Il avait été admis à l'AEIS en mars 2016 .

Nous regretterons tous sa disparition et nous transmettons à son épouse toutes nos condoléances.

Documents

Notre Collègue Juan Carlos CHACHQUES nous fait part de sa publication de deux de ses articles:

p 08 :paru dans la revue *European Journal of Cardio-Thoracic Surgery* 0 (2019) 1–11 du 20 septembre 2019 , : un article intitulé *Elastomeric cardiopatch scaffold for myocardial repair and ventricular support* par Juan Carlos Chachques et al.

p 19 : paru dans la revue Cells **2019**, 8, 166; doi:10.3390/cells8020166 du 17 févier 2019, , accessible sur le site https://www.mdpi.com/journal/cells , intitulé *Exosome in Cardiovascular Diseases: A Complex World Full of Hope,* par Juan Carlos Chachques et al.

Elastomeric cardiopatch scaffold for myocardial repair and ventricular support

Juan Carlos Chachques[a,*], Nermine Lila[a], Carolina Soler-Botija[b,c], Cristina Martinez-Ramos[d], Ana Valles [d], Gwennhael Autret[e], Marie-Cecile Perier[f], Nicolas Mirochnik[g], Manuel Monleon-Pradas[d], Antoni Bayes-Genis[b] and Carlos E. Semino[h]

[a] Laboratory Biosurgical Research, Alain Carpentier Foundation, Cardiac Surgery Pompidou Hospital, University Paris-Descartes, Paris, France
[b] Research Cardiology Institute, Germans-Trias-Pujol Hospital, Badalona, Spain
[c] CIBER Cardiovascular, Carlos III Health Institute, Madrid, Spain
[d] Center for Biomaterials and Tissue Engineering, Polytechnic University Valencia, Valencia, Spain
[e] Microcirculation Imaging Lab, Paris Cardiovascular Research Center (PARCC), University Paris, Paris, France
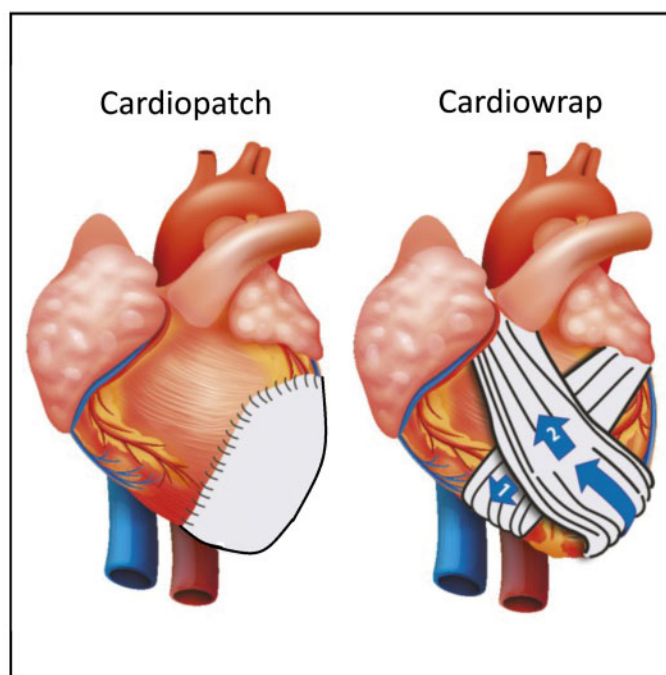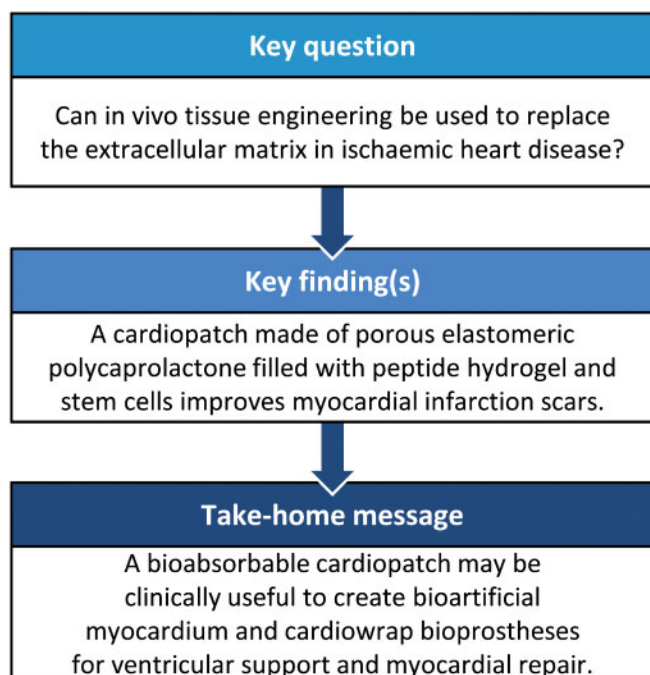[f] Cardiovascular Epidemiology Unit, PARCC, University Paris, Paris, France
[g] Cardiology Department, Pompidou Hospital, University Paris, Paris, France
[h] Bioengineering Department, IQS-School Engineering, Ramon-Llull University, Barcelona, Spain

* Corresponding author. Biosurgical Research Laboratory, Alain Carpentier Foundation, Cardiac Surgery Pompidou Hospital, 56 rue Leblanc, 75015 Paris, France. Tel: +33-613144398; fax: +33-156095903; e-mail: j.chachques@aphp.fr (J.C. Chachques).

Key question

Can in vivo tissue engineering be used to replace the extracellular matrix in ischaemic heart disease?

Key finding(s)

A cardiopatch made of porous elastomeric polycaprolactone filled with peptide hydrogel and stem cells improves myocardial infarction scars.

Take-home message

A bioabsorbable cardiopatch may be clinically useful to create bioartificial myocardium and cardiowrap bioprostheses for ventricular support and myocardial repair.

Abstract

OBJECTIVES: Prevention of postischaemic ventricular dilatation progressing towards pathological remodelling is necessary to decrease ventricular wall deterioration. Myocardial tissue engineering may play a therapeutic role due to its capacity to replace the extracellular matrix, thereby creating niches for cell homing. In this experimental animal study, a biomimetic cardiopatch was created with elastomeric scaffolds and nanotechnologies.

METHODS: In an experimental animal study in 18 sheep, a cardiopatch was created with adipose tissue-derived progenitor cells seeded into an engineered bioimplant consisting of 3-dimensional bioabsorbable polycaprolactone scaffolds filled with a peptide hydrogel (PuraMatrix™). This patch was then transplanted to cover infarcted myocardium. Non-absorbable poly(ethyl) acrylate polymer scaffolds were used as controls.

RESULTS: Fifteen sheep were followed with ultrasound scans at 6 months, including echocardiography scans, tissue Doppler and spectral flow analysis and speckle-tracking imaging, which showed a reduction in longitudinal left ventricular deformation in the cardiopatch-treated group. Magnetic resonance imaging (late gadolinium enhancement) showed reduction of infarct size relative to left ventricular mass in the cardiopatch group versus the controls. Histopathological analysis at 6 months showed that the cardiopatch was fully anchored and integrated to the infarct area with minimal fibrosis interface, thereby promoting angiogenesis and migration of adipose tissue-derived progenitor cells to surrounding tissues.

CONCLUSIONS: This study shows the feasibility and effectiveness of a cardiopatch grafted onto myocardial infarction scars in an experimental animal model. This treatment decreased fibrosis, limited infarct scar expansion and reduced postischaemic ventricular deformity. A capillary network developed between our scaffold and the heart. The elastomeric cardiopatch seems to have a positive impact on ventricular remodelling and performance in patients with heart failure.

Keywords: Heart failure • Cardiac tissue engineering • Elastomeric scaffold • Cardiopatch • Cardiowrap • Translational and clinical research

---

ABBREVIATIONS	
CLMA	Cross-linked polycaprolactone
3D	3-Dimensional
ECM	Extracellular matrix
LV	Left ventricular
MI	Myocardial infarction
MMP9	Metalloproteinase 9
PEA	Poly(ethyl) acrylate

INTRODUCTION

Extracellular matrix (ECM) remodelling in heart failure (excessive matrix degradation and myocardial fibrosis) contributes to left ventricular (LV) dilatation and progressive cardiac dysfunction. An appropriate balance of ECM synthesis and degradation is required for normal morphogenesis and maintenance of tissue architecture. In ischaemic heart disease, the imbalance in the ECM turnover either by decreased matrix synthesis and/or increased degradation leads to cardiac dilatation or infarct rupture [1–4]. Myocardial tissue engineering should provide structural support to the heart; specific scaffolds should help to normalize cardiac wall stress in injured regions by improving strain distribution [1, 5, 6]. Engineering materials requiring specific properties of stiffness and resistance to deformation can be implanted around the heart or seeded into the myocardial tissue. They are composed of a natural or synthetic structure capable of supporting 3-dimensional (3D) tissue formation. Scaffold characteristics are critical to recapitulating the *in vivo* milieu and allowing cells to influence their own microenvironments. Such scaffolds serve the following purposes: allow cell attachment and migration, deliver and retain cells and biochemical factors, enable diffusion of vital cell nutrients and expressed products and exert certain mechanical and biological influences to modify the behaviour of the cell phase [1, 5, 7].

The objective of this *in vivo* tissue engineering study was to assess the safety and efficacy of 3D scaffold cardiopatches in an myocardial infarction (MI) sheep model with pathophysiological and biomechanical degradation similar to that seen in humans. The cardiopatches were created using elastomeric porous membranes filled with nanometric self-assembling peptides seeded with autologous adipose tissue-derived progenitor cells (ATDPCs) and grafted onto LV MI scars.

MATERIALS AND METHODS

In 18 Île-de-France sheep weighing 36.2 ± 5.3 kg, MIs were created with surgical occlusion of the left anterior descending diagonal coronary artery branches. Two months later, the MI was surgically treated either with semidegradable or with non-degradable cardiopatches made of elastomeric membranes filled with self-assembling peptide-RAD16-I Puramatrix™ (BD Biosciences, Franklin Lakes, NJ, USA) seeded with ATDPCs (Fig. 1A and B). A third control group had MIs without treatment.

All experiments were performed at the Laboratory of Biosurgical Research (ISO-Certification 9001), Pompidou Hospital, University of Paris Descartes, Paris, France, and received care in compliance with the European Conventions. Animal studies were approved by the ethics committee for animal research of Paris Descartes University, France.

Technique of experimental myocardial infarction

Preoperative management, anaesthesia procedure and postoperative care were performed consistent with our previously described experimental studies [7].

A median sternotomy was performed, and the pericardial sac was opened exposing the heart. To reduce the risk of ventricular fibrillation, xylocaine 1% (Lidocaine, AstraZeneca, Cambridge, UK) was continuously infused intravenously (2 mg/kg per hour) during the surgical procedure. Mediastinal fat tissue was harvested for isolation and expansion of ATDPCs.

An MI was created by ligation of the diagonal branches of the left anterior descending coronary artery using 5-0 non-absorbable Prolene sutures. Significant electrocardiographic changes, including widening of the QRS complex, elevation of the ST segment and colour and kinetic changes of the anterior wall were considered indicative of coronary occlusion. Transepicardial echocardiography was performed before and after the MI to assess ventricular dimensions and function and to identify the infarcted area.
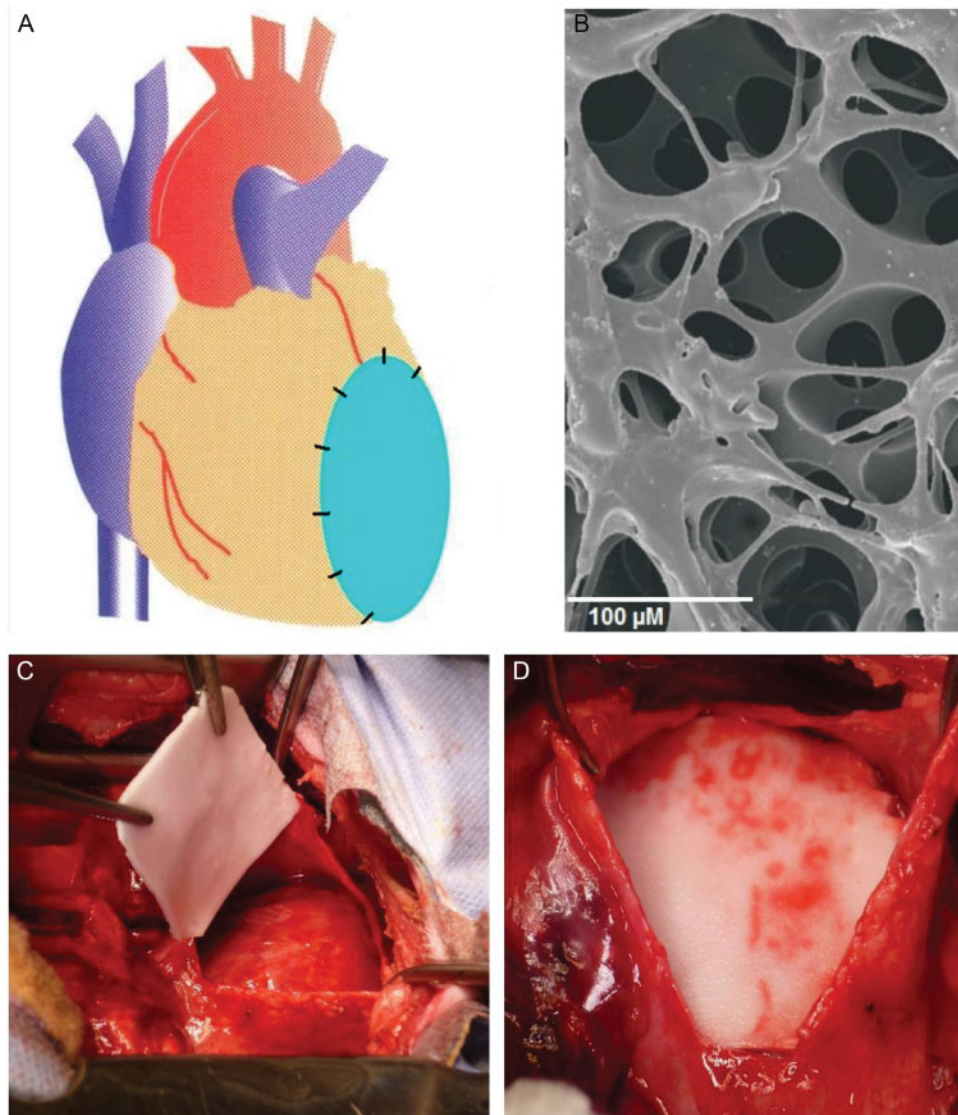
Figure 1: Elastomeric scaffolds for the treatment of chronic myocardial infarction. The cardiopatch is created with porous elastomers filled with nanometric peptides containing adipose tissue-derived progenitor cells (**A** and **B**). The cardiopatch was surgically grafted on sheep left ventricular infarct scars (**C** and **D**).

Isolation, culture and transduction of adipose tissue-derived progenitor cells from sheep

Cells were isolated from mediastinal adipose tissue by 0.05% collagenase II digestion at 37°C and adhesion to the plate surface in α-minimum essential medium supplemented with 10% foetal bovine serum and 1% penicillin-streptomycin. ATDPCs were cultured under standard conditions (37°C, 5% CO_2) (duplication time 0.7 days) and labelled with CMVp-RLuc-mRFP1 lentivirus (2×10^6 transduction units/ml; MOI = 21) for 48 h. The highest 11% RFP-expressing cells were selected by FACS (Fluorescence-Activated Cell Sorting) to be used for implantation. Cells were then expanded to 100 ± 7 million and loaded into cardiopatch scaffolds.

Preparation of cardiopatches

Scaffold membranes consisted of a matrix with large-sized spherical pores (130 ± 20 μm) with good interconnectivity obtained by a porogenic template-manufacturing technique (Fig. 1B). Sintered microbeads with a narrow distribution of diameters were used as a polymerization template and eliminated after polymerization of the matrix precursors in its interstices. The pores of the scaffolds were filled with PuraMatrix hydrogel 1% (w/v), which is capable of forming fibrillar structures in the range of nanometers [8].

Two different bioactive patches were developed:

1. *Semidegradable* elastomeric porous membranes made from interpenetrating polymer networks of cross-linked hyaluronic acid and cross-linked polycaprolactone (CLMA). They are partially reabsorbed leaving a residual permanent light skeleton for mechanical support (Fig. 1) [9, 10].
2. *Non-degradable* elastomeric porous membranes from poly(-ethyl) acrylate (PEA) polymer filled with Puramatrix peptide hydrogel using a gentle vacuum.

Treatment with the cardiopatch (2 months after infarct)

General anaesthesia was readministered via the same protocol used for the MI model. The LV was accessed via a left thoracotomy through the 5th intercostal space.

Sheep were randomized into 3 treatment groups: group 1 ($n = 5$) had MIs without treatment (control group); group 2 ($n = 5$) had MIs treated with a CLMA patch; group 3 ($n = 5$) had MIs treated with the PEA patch.

Implantation of cardiopatches

The elastomeric membranes measured 50×50 mm and were 2 mm thick; all were seeded with ATDPCs and placed onto the surface of the LV, then fixed to the epicardium with interrupted superficial sutures (Prolene 5-0 placed at the periphery of the cardiopatch) (Fig. 1).

Evaluation at 6 months with echocardiography, magnetic resonance imaging and histopathological examination

With the sheep under general anaesthesia, a redo sternotomy was performed. Transepicardial echocardiography was then carried out followed by magnetic resonance imaging (MRI) with an injection of an intravenous gadolinium solution at a dose of 0.4 ml/kg. The animals were then sacrificed by a lethal intravenous injection of Dolethal (pentobarbital sodium 200 mg/ml) (Vetoquinol, Lure, France).

Transepicardial echocardiography

A MyLab30-Gold cardiovascular ultrasound system (Esaote S.p.A., Firenze, Italy) equipped with a phased-array 1–5 MHz transducer was used to assess (i) LV end diastolic volume-end systolic volume, stroke volume, shortening fraction and ejection fraction; (ii) Doppler spectral flow for peak E deceleration time, A-wave, LV outflow tract-velocity time integral; and (iii) tissue Doppler for peak velocities of the mitral annulus in early (E') phases of LV filling (measured at the lateral portion of the mitral annulus); the dimensionless ratio E/E' was computed. For each scan, 1 cardiac cycle was acquired at a frame rate of 60–70 Hz. Deformation of the ventricular wall was evaluated by longitudinal strain using speckle-tracking based analysis [11].

Magnetic resonance imaging

A BioSpec 47/40 USR system (Bruker-Corp., Karlsruhe, Germany) was used for MRI studies. The extracellular MRI contrast medium gadolinium allowed detection of infarct scars by late-hyperenhancement of the scar tissue. Immediately after autopsy, the isolated sheep hearts underwent *ex vivo* MRI to assess the infarct size (gadolinium white-marked areas) relative to myocardial mass and the integration of the cardiopatch onto the ventricular wall [12]. Three-dimensional evaluations were performed using longitudinal and transverse MRI serial planes (Fig. 2).

Histopathological studies

All sheep were sacrificed at 6 months. The site of the myocardial injury was identified and dissected with 4–5 specimens taken and fixed in 10% formalin, embedded in paraffin and sectioned into 10-μm-thick slices. The sections were stained with haematoxylin–eosin–saffron, Masson trichrome and Sirius red stains. A polarized light microscope was used to measure collagen types I and III on randomly selected Sirius red-stained sections from both infarct and border zones. To identify the grafted cells, sections were incubated with antibodies against cardiac troponin I and RFP (2 μg/ml; Abcam, Cambridge, UK). Immunostaining against metalloproteinase 9 (MMP9; 10 μg/ml; Chemokine Therapeutics Corp, Vancouver, BC, Canada) was also performed. Nuclei were counterstained with 4′,6-diamidino-2-phenylindole (Thermo Fisher Scientific, Waltham, MA, USA), and the results were analysed with an Axio-Observer Z1 (Zeiss, Oberkochen, Germany) laser confocal microscope. To determine vessel density, heart sections were stained with biotinylated GSLI B4 isolectin (Vector Laboratories, Burlingame, CA, USA), and Alexa 647-conjugated streptavidin (ThermoFisher). Images were taken in 10 randomly selected fields (5 infarcted areas + 5 remote healthy areas) and analysed using ImageJ software (available at https://imagej.nih.gov/ij/). Results were expressed as a percentage of the mean isolectin-positive area per area of tissue surface.

Statistical analysis

Statistical analyses were performed with SPSS Statistics version 19 (IBM Corporation, Armonk, NY USA). Results were analysed and reported as percentage or mean ± standard deviation or median interquartile range when appropriate. Differences between groups were compared using the Student's *t*-test or one-way analysis of variance for multiple comparisons. A *P*-value of <0.05 was considered to be statistically significant. Comparisons of echocardiography and MRI parameters across treatment groups were performed using analysis of variance and the non-parametric Kruskal–Wallis test.

RESULTS

There were 3 surgical complications and 1 animal died during the infarct induction procedure of irreversible ventricular fibrillation. Two animals were excluded from the study due to skin and mediastinal infections. In summary, 15 sheep survived (5 for each study group) and were evaluated over the long term.

Echocardiography

LV function and dimensions were quantified the day of the myocardial infarction. Only animals developing LV dysfunction with an ejection fraction less than 35% gained access to the second phase. At the 6-month follow-up examination, the attenuated parameters of ventricular deformation observed in the cardiopatch groups were assessed with speckle-tracking imaging (longitudinal strain). Diastolic function was improved (E deceleration time assessment) in treated groups versus controls. Significant benefits were also observed in the following ultrasound parameters: E/A ratio, E/E' ratio, LV outflow tract-velocity time integral (Table 1).

Magnetic resonance imaging

The white tonality of infarct scars is enhanced vividly 15 min after the administration of intravenous gadolinium, representing the accumulation of gadolinium in the extracellular space due to the
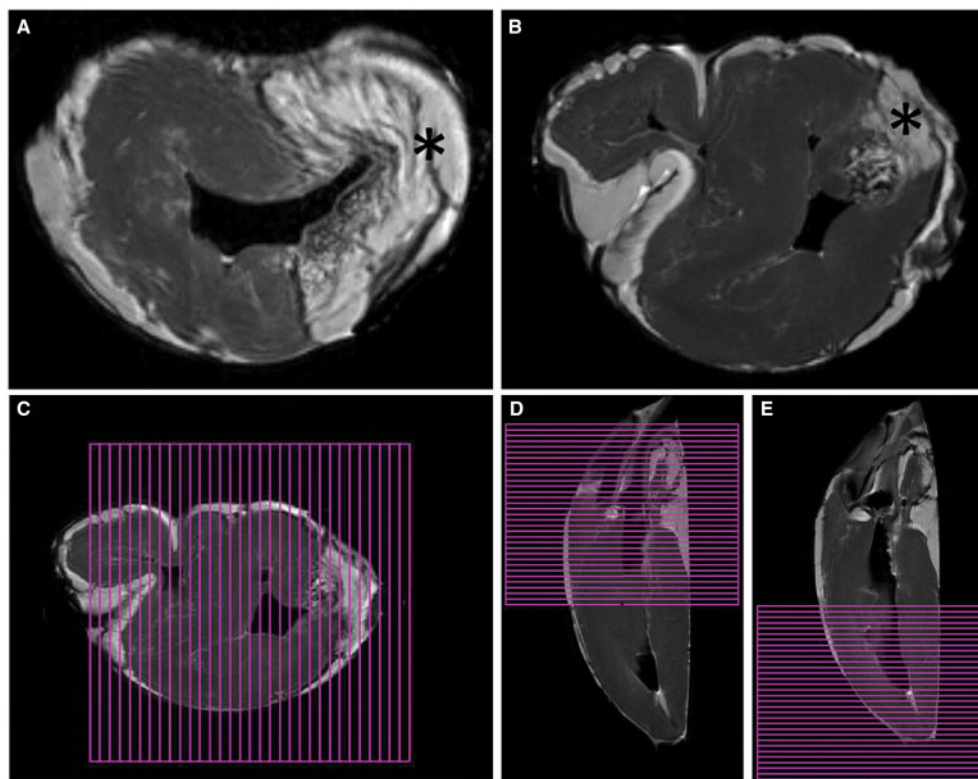
Figure 2: Cardiopatch evaluation with magnetic resonance imaging. Hyperenhancement on the infarct scar with the contrast medium gadolinium (signals in white). (**A**) Transverse left ventricular imaging showing large myocardial infarction (asterisk) in a control untreated sheep. (**B**) Magnetic resonance imaging showing reduced infarcted area (asterisk) in CLMA cardiopatch-treated sheep (both at 6-month follow-up). (**C–E**) Three-dimensional evaluation of myocardial mass and infarct size using transverse and longitudinal serial planes.

loss of membrane integrity in the infarcted tissue. At the 6-month follow-up examination, CLMA patches were more adherent to and integrated into the ventricular wall compared with the PEA patches. The volume of the infarct scars related with the ventricular mass showed a significant reduction of the relative infarct volume in the cardiopatch-treated group, mainly in the CLMA group (Fig. 2; Table 2).

Left ventricle histopathology

The surgical coronary artery ligation model for this study results in the transmural necrosis of the LV wall with central fibrosis and an intermediate border zone surrounded by healthy myocardium. In the cardiopatch-treated sheep, mainly in the CLMA group, the necrotic areas were significantly less prominent than in the non-treated control group (Fig. 3). To further investigate this observation, collagen content was measured in the infarcted regions and in the healthy myocardium bordering the infarcts. At sacrifice, the collagen volume fraction in the infarct core was $37.6 \pm 3.7\%$, $25.3 \pm 7.0\%$ and $35.4 \pm 5.2\%$ in the controls, the PEA and the CLMA-treated animals, respectively ($P = 0.01$). Collagen type I accounted for only 14.5% of ECM in the PEA-treated animals whereas it increased to 27.1% and 28.5% of total collagen in the controls and in the CLMA-treated group, respectively ($P = 0.001$). Collagen III contents did not present with statistical differences in any of the groups ($P = 0.06$). Collagen volume fraction values were also similar in the border regions with $4.7 \pm 3.5\%$, $2.1 \pm 1.1\%$ and $2.9 \pm 2.0\%$ in the controls and in the PEA- and CLMA-treated animals, respectively ($P = 0.24$).

Expression of MMP9 was also analysed due to its possible role in the degradation of ECM and in myocardial remodelling. Immunostaining against MMP9 in all the experimental groups revealed the presence of MMP9-positive inflammatory cells in infarct, border and remote zones (Fig. 4). Animals treated with the PEA membrane had a statistically significantly lower quantity of MMP9-expressing cells in border and remote areas ($P < 0.001$ and $P = 0.005$, respectively). CLMA-treated animals, however, presented with a higher number of MMP9-positive cells in the border zone ($P = 0.002$) (Fig. 4).

ATDPCs positive for RFP were found inside the patch and in the infarct scars and healthy myocardium in both treated groups (Fig. 5A–H). Hence, ATDPCs were able to migrate from the cardiopatch to the nearby tissue (Fig. 5A and E). Integration of ATDPCs into the vessel structures was also observed in the cardiopatch interconnected with myocardium (Fig. 5B and F). ATDPCs therefore contributed to the formation of a capillary network between the cardiopatch and the myocardium (Fig. 5C, D, G and H).

Evaluation of vessel density revealed a greater percentage of vessels in the infarcted areas in animals treated with CLMA patches compared to the controls and the PEA-treated groups (1.17 ± 0.27, 0.70 ± 0.09 and 0.68 ± 0.09, respectively) with statistically significant differences (CLMA vs controls, $P = 0.025$; CLMA vs PEA, $P = 0.019$) (Fig. 6). No differences in vessel density were observed between the controls and the PEA-treated animals in infarct zones or in border myocardium. These results suggest that CLMA patches, together with implanted ATDPCs, may promote the formation of new vessels in the ischaemic myocardium.

Table 1: Echo Doppler studies: 6-month follow-up

	Control		CLMA		PEA		
	n	Mean (SD) or median (interquartile range)	n	Mean (SD) or median (interquartile range)	n	Mean (SD) or median (interquartile range)	P-value[a]
SL	5	2.2 ± 0.5	5	4.7 ± 1.2	5	7.3 ± 1.6	0.04
DD (mm)	5	42.14 ± 7.67	5	43.33 ± 4.76	5	38.40 ± 3.21	0.37
SD (mm)	5	31.00 ± 6.48	5	30.67 ± 4.32	5	25.80 ± 3.27	0.20
EF (%)	5	52.00 ± 9.06	5	56.17 ± 6.01	5	61.40 ± 9.79	0.19
SF (%)	5	26.71 ± 5.62	5	32.50 ± 9.83	5	32.80 ± 6.91	0.3
E/A ratio	5	1.53 ± 0.31	5	1.35 ± 0.34	5	1.04 ± 0.32	0.06
EDT (ms)	5	118.14 ± 23.2	5	132.50 ± 31.5	5	147.80 ± 27.42	0.04
E/E' ratio	5	5.10 ± 1.3	5	3.50 ± 0.9	5	4.30 ± 1.2	0.03
VTI (cm)	5	9.71 ± 1.80	5	12.00 ± 2.00	5	11.2 ± 1.9	0.07
SV (mL)	5	17.02 ± 4.3	5	23.79 ± 5.21	5	24.02 ± 3.7	0.28

[a]*P*-value for analysis of variance or Kruskal–Wallis test across the 3 groups.
CLMA: polycaprolactone; DD: left ventricular diastolic diameter; *E/A* ratio: mitral inflow velocities, peak early filling (E-wave) and late diastolic filling (A-wave); EDT: E deceleration time; EF: ejection fraction; PEA: poly(ethyl) acrylate; SD: left ventricular systolic diameter; SF: shortening fraction; SL: longitudinal strain; SV: stroke volume; VTI: left ventricular velocity time integral.

Table 2: Magnetic resonance imaging: 6-month follow-up of myocardial size/left ventricular mass

Group	LV myocardial mass, cm³	3-Dimensional infarct size, cm³	Infarct size/LV myocardial mass, %
Control	98.7 ± 12.9	13.8 ± 4.7	13.9 ± 2.3
CLMA patch	102.2 ± 14.4	6.4 ± 1.6	6.3 ± 1.1[a]
PEA patch	102.0 ± 11.9	10.1 ± 5.7	9.9 ± 4.8[a]

Data are expressed as mean (standard deviation).
[a]*P* < 0.05 versus control group, adjusted for multiple testing (Tukey adjustment).
CLMA: polycaprolactone; LV: left ventricular; PEA: poly(ethyl) acrylate.

At the level of the epicardium, we found a minimal fibrosis interface without inflammation between both the cardiopatch and the heart surface. The CLMA patch was completely anchored to and incorporated into the nearest infarct area and the myocardium. In contrast, the PEA patches macroscopically showed poor adhesions to the heart and the infarct scar although some areas were nicely attached to the myocardium (Fig. 5D). Overall, the bioabsorbable CLMA patches possessed improved flexibility and adapted better to the curvature of the heart's surface than did the biostable hydrophobic PEA patches.

DISCUSSION

Results of isolated stem cell therapy in cardiac diseases showed that cell bioretention and engraftment within infarcts are low because cell homing is limited by the degradation of the ECM, resulting in adverse LV remodelling [2–4, 13]. The association of elastomeric scaffolds with stem cells raises the possibility of repairing the damaged myocardial tissue and avoiding ventricular chamber dilation. The cardiopatch seems appropriate to support MI scars by a 'Band-Aid' effect, limiting the spread of the infarcted areas and improving the ventricular wall by minimizing stress tolerance by a girdling effect [7].

Cardiowrap–biological ventricular support

The first biomechanical strategy limiting ventricular dilatation was the latissimus dorsi dynamic-cardiomyoplasty for patients with severe heart failure awaiting a heart transplant [14]. More than 2000 patients have been operated on worldwide; cardiomyoplasty provides an autologous source of circulatory assistance. The chronically electrostimulated latissimus dorsi skeletal muscle flap wrapped around the heart works in concert with the myocardium, improving the haemodynamics via an electronic cardiomyostimulator device with electrodes. Less invasive alternative approaches like ventricular restraint therapy using polyester mesh wraps and nitinol devices have been proposed for patients with heart failure; however, these constraint acellular devices have failed to demonstrate clear clinical benefits [15]. A new approach based on myocardial tissue engineering might instead herald myocardial healing and evidence of ventricular support [5].

The main purpose of the cardiopatch is to display structural and functional properties similar to those of natural extracellular matrices containing 3D nanostructures and proper instructive niches for cell homing [8–10]. Speckle-tracking ultrasound revealed positive results about deformation of the LV and improvements in patients with MI treated with a cardiopatch versus a control group. MRI analysis of the infarct area using serial planes showed significant reduction of the infarct scar in the cardiopatch-treated groups [11, 12].

Histopathologically, matrix metalloproteinases are endopeptidases that cleave all components of the ECM and participate in LV remodelling [16]. In particular, MMP9 is important because upregulation after the MI and gene deletion attenuate LV remodelling [17]. Furthermore, studies of infarct rupture have also demonstrated that MMP9 is expressed by inflammatory cells in the infarcted area [17]. The biodegradable characteristics of the CLMA cardiopatch may induce a greater inflammatory effect, thereby increasing the number of MMP9-positive cells. Thus, the elevated density of the vessel may facilitate cell mobilisation in an MI treated with CLMA. The presence of ATDPCs in the scar and in the healthy myocardium seems to indicate that the
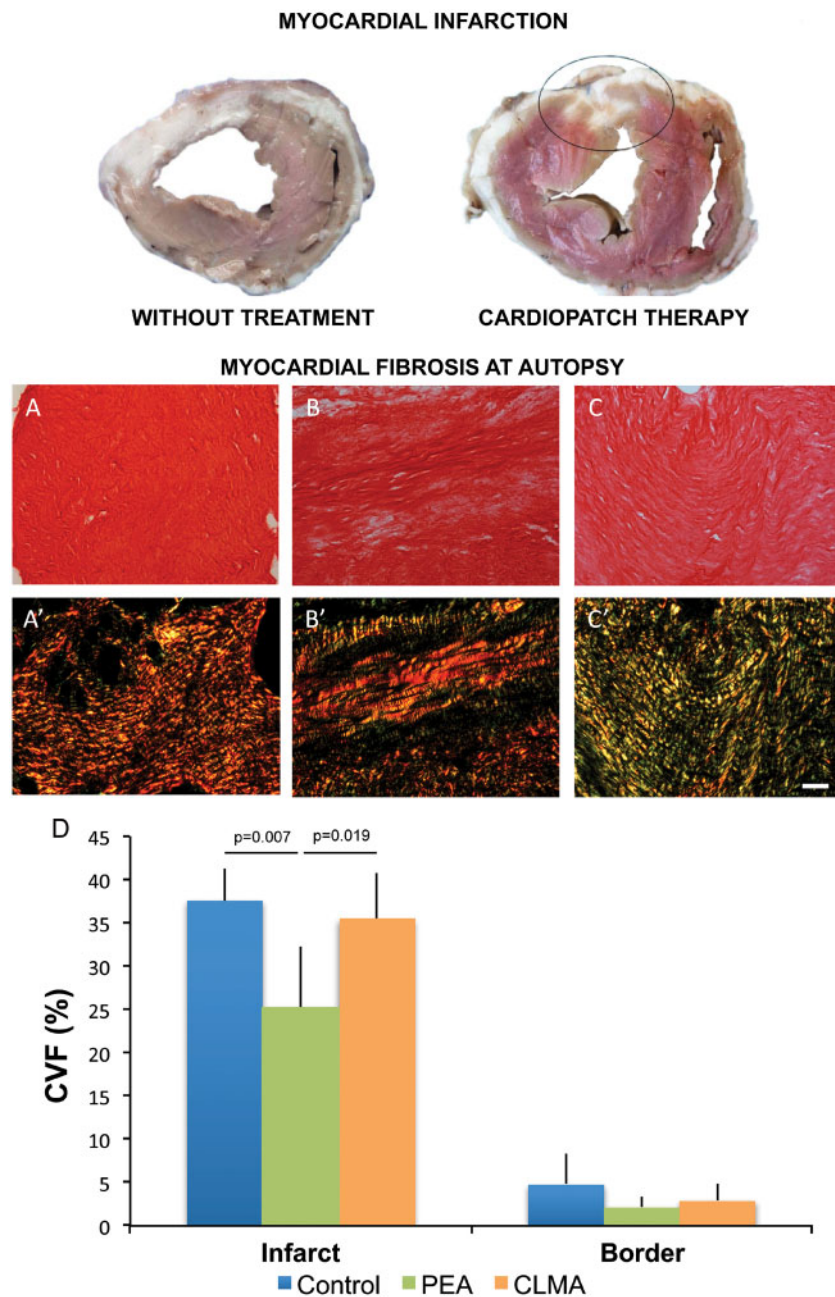
Figure 3: Macroscopic pathology of sheep ventricles showing white scars of myocardial infarction at 6 months. (**Upper left**) Control untreated heart with large infarct scar. (**Upper right**) Reduced size of infarct scar in sheep treated with CLMA cardiopatch (encircled area). (**Lower pictures**) Evaluation of myocardial fibrosis at autopsy. Sirius red staining distinguishing collagen (red) in infarct zones from control (**A**), CLMA (**B**) and poly(ethyl) acrylate (**C**) groups. (**A'–C'**) Polarized light microscopy images exhibit collagen I (red/yellow) and collagen III (green) fibrils in the same sections. Scale bar 50 μm. (**D**) CVF in percentage measured on polarized light images. Results are presented as the mean percentage of CVF. Error bars: ±standard deviation. *P*-value <0.05 was considered significantly different. CLMA: cross-linked poly-caprolactone; CVF: collagen volume fraction; PEA: poly(ethyl) acrylate.

implanted ATDPCs are able to migrate from the cardiopatch to the nearby cardiac tissue, possibly promoting angiogenesis. This outcome was suggested in a previous study in which human ATDPCs loaded in CLMA patches expressed cardiac troponin I when implanted in a mouse model of MI [10].

Complete vascularization of implanted CLMA and PEA patches was also demonstrated in addition to vascular connections in the myocardial–cardiopatch interface. This finding is important for cell survival and for the proper integration of the bioactive implant over the cardiac tissue. The composition of the patches and

the peptide hydrogel RAD16-I facilitated capillary formation and distribution, as was previously experimentally shown *in vitro* [18]. Interestingly, ATDPCs were integrated in some of those vessels, thereby contributing to the capillary network. This finding was also observed in human ATDPCs implanted via a fibrin patch in a murine MI model [19].

Analysis of vascular density revealed an increase in the percentage of the vascular area in the infarcted zones when animals were treated with CLMA patches and ATDPCs compared to those treated with PEA and the controls. The channelled structure and
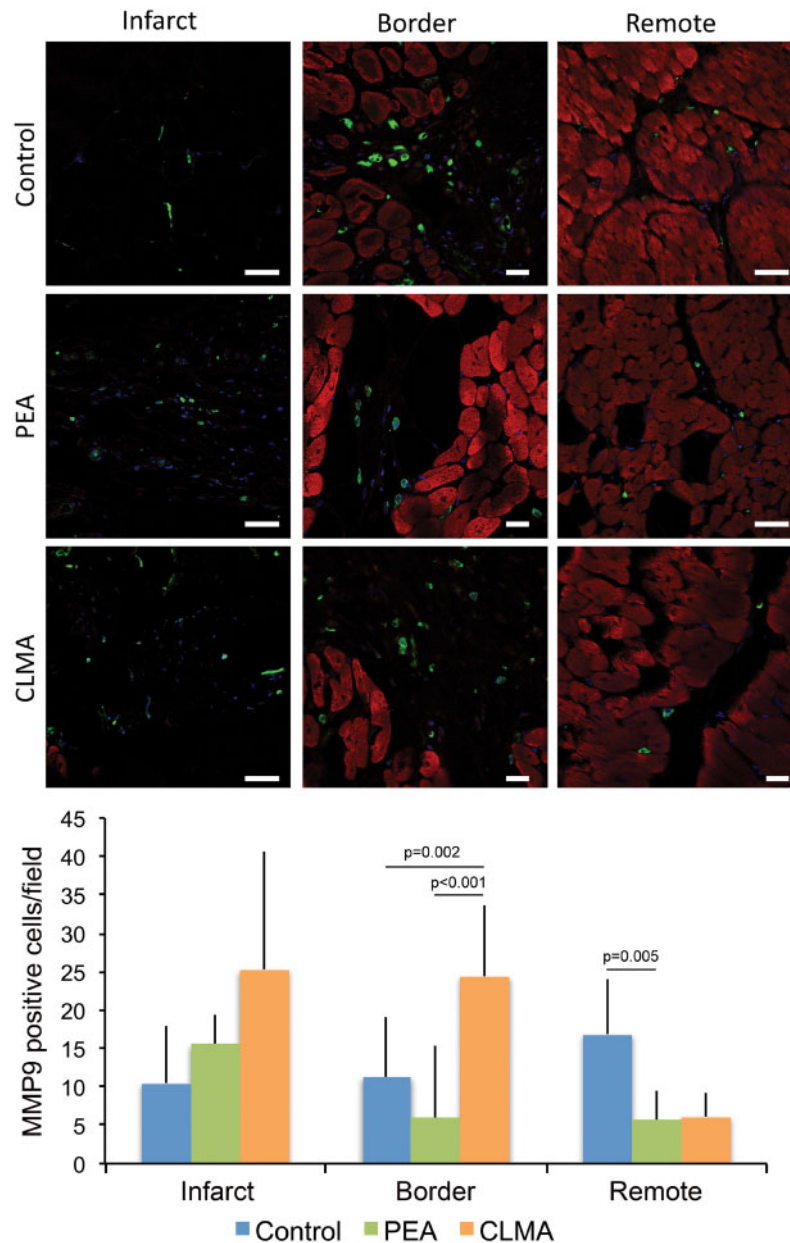
Figure 4: Immunodetection of MMP9 in control, PEA and CLMA-treated animals. MMP9 (green), cardiac troponin I (red) and nuclei (4′,6-diamidino-2-phenylindole, blue). Scale bars 50 mm. Histogram of the number of MMP9-positive cells per field in infarct, border and remote zones. Results are presented as the mean number of MMP9-positive cells per field ± standard deviation. *P*-value <0.05 was considered significantly different. CLMA: cross-linked polycaprolactone; MMP9: metalloproteinase 9; PEA: poly(ethyl) acrylate.

progressive biodegradation characteristics of the CLMA patches might facilitate the diffusion of the proangiogenic factors from the patch to the myocardium more easily than the PEA biostable patches.

Clinical translation

The first clinical application of *in vivo* myocardial tissue engineering was the MAGNUM (Myocardial Assistance by Grafting a New bioartificial Upgraded Myocardium) trial in 2007. In this study, a collagen type I cardiopatch seeded with mononuclear bone marrow cells was grafted onto LV MI scars [20]. In this example of *in vivo* tissue engineering, the body is the bioreactor.

The lack of adequate tensile properties and the lack of controlled bioresorption of collagen cardiopatch boosted our interest for the use of elastomer scaffolds and nanofibres, creating a cardiopatch-like bioartificial myocardium. This novel cardiac repair strategy included a porous elastomeric 3D polycaprolactone cardiopatch filled with Puramatrix-containing stem cells, which mimics the biophysical and biomechanical attributes of natural myocardium.

Our study demonstrates the feasibility and effectiveness of a cardiopatch grafted onto MI scars in large animals. This treatment reduced infarct volume and fibrosis, limited ventricular deformation and improved ventricular function. There was minimal fibrosis interface with minimal inflammation between the heart and the patch. The cardiopatch was firmly anchored and
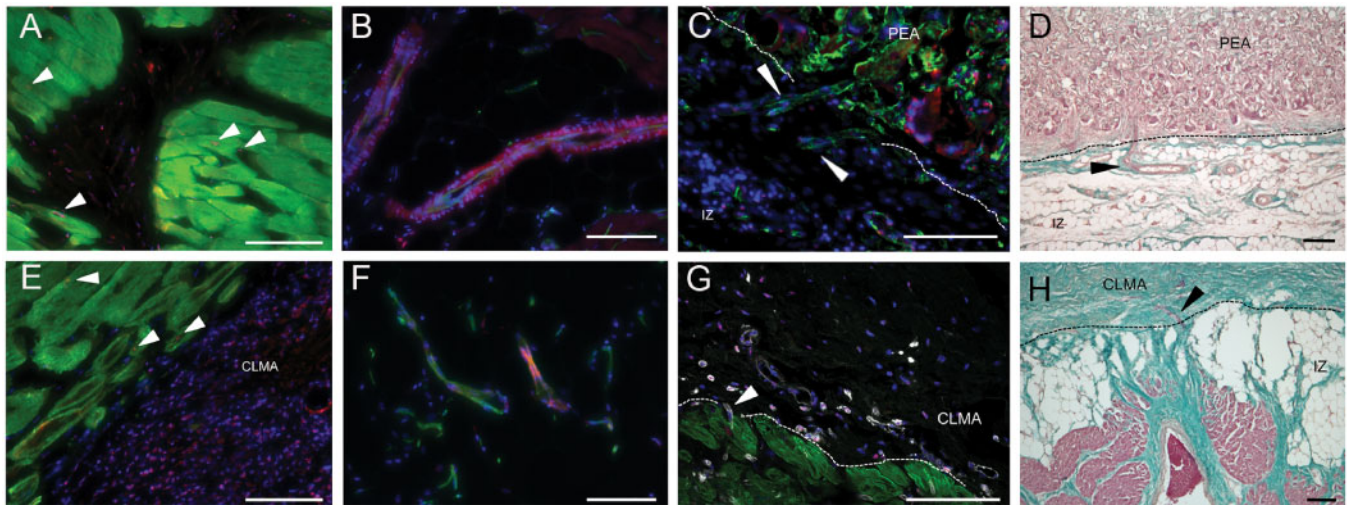
Figure 5: Immunostaining of heart sections. Sheep infarcted hearts treated with adipose tissue-derived progenitor cells (ATDPCs) (red) loaded in PEA (**A–D**) or CLMA cardiopatches (**E–H**). (**A** and **E**) Presence of ATDPCs (red, arrowheads) in the myocardium [cardiac troponin I (cTnI), green]. (**B, C** and **F**) Presence of vessels (green) in the cardiopatches and integration of ATDPCs in the vessels (magenta). (**G**) Vessels (white), cTnI (green) and ATDPCs (red) staining. Nuclei (4′,6-diamidino-2-phenylin-dole, blue). (**D** and **H**) Masson's trichrome staining of heart sections. Arrowheads in **C**, **D**, **G** and **H** indicate vascular connections. Scale bars 100 μm in **A–C**, **E–G** and 200 μm in **D** and **H**. CLMA: cross-linked polycaprolactone; IZ: infarcted zone; PEA: poly(ethyl) acrylate.

integrated to the infarct area and the myocardium; it promoted new vessel formation in ischaemic myocardium; it reduced the number of inflammatory cells expressing MMP9; and, therefore, reduced adverse cardiac remodelling and the risk of postinfarct ventricular rupture [16, 17].

Perspectives

Cardiopatch biotechnology might be applied to the creation of cardiowrap bioprostheses for external ventricular support with myocardial repair, thereby reducing progression to heart failure and the indication for a heart transplant. The proposed ventricular support bioprostheses are manufactured with elastomeric polycaprolactone membranes (helical bands) to avoid progression of adverse ventricular remodelling (see Supplementary data: Invention Patents Chachques et al. 'Bioactive implants for myocardial regeneration and ventricular chamber restoration': US Patent 8 968 417 B2, 2015; US Patent Part2 10 004 602 B2, 2018; European Patent 2 422 823 B1, 2014).

The design of the ventricular support bioprostheses is based on the concept of the 'helical myocardial band', which describes the anatomical configuration of the heart, whereby muscular ventricular bands provide conical configuration to the LV chamber (Torrent-Guasp concept). The role of the myocardial band is to limit ventricular dilatation, preserving elliptical shape and contributing to systolic contraction and diastolic filling (suction mechanism).

A ventricular support bioprosthesis is used to wrap the ventricles, starting near the left atrial appendage at the level of the pulmonary artery root and ending at the level of the aortic root. The loop/band can be affixed onto the heart and/or onto the cardiopatch by surgical sutures, biological or synthetic glue or surgical clips.

Future cardiowrap scaffolds might be manufactured using 3D printing [21] and new functionalization strategies, focusing on nanocontainer technology for the sustained release of active molecules (basic fibroblast growth factor, vascular endothelial growth factor, epidermal growth factor). The nanocontainers are fixed onto poly(ε-caprolactone) fibres, which improve tissue repair [22]. Another approach to enhance the bioactivity of the scaffolds is to graft poly(sodium styrene sulfonate) onto poly(ε-caprolactone) membranes [23]. The implantation of a poly-L-lactide granulocyte colony-stimulating factor-functionalized scaffold in a rabbit model of chronic MI induced an angiogenetic process and the reorganization of the ECM architecture leading to connective tissue deposition and scar remodelling [24].

Limitations

To avoid the risk of death related to exposure to general anaesthesia and heart manipulation during dissection of the infarct scar area, the animals in group 1 did not have a sham operation at 2 months.

Our surgical MI was created by ligation of diagonal branches of the left anterior descending artery. This procedure results in a segmental dysfunction of the anterior and lateral walls without malignant ventricular arrhythmias, thereby avoiding massive LV failure, which results in a high operative mortality rate in sheep [25]. Surgical induction of infarcts in the diagonal area of the LV also may not be clinically relevant because of the small infarct territory. Moreover, catheter-based MI models are still associated with a high mortality rate [25]. In accordance with the regulations of our university ethics committee, research projects using large-animal models must strictly abide by the rules related to the minimum necessary number of groups and interventions to evaluate new surgical procedures and to satisfy statistical requirements.

The MRI system available in our research centre only allowed evaluation of small animals (rabbit, rats, mice). For this reason, we performed ex vivo MRI evaluation of the sheep hearts at 6 months to measure MI volumes. Procedures included removing the hearts after the last echocardiographic assessment and 15 min after administering intravenous injections of gadolinium. The sheep were given general anaesthesia and an overdose of the anaesthetic pentobarbital.
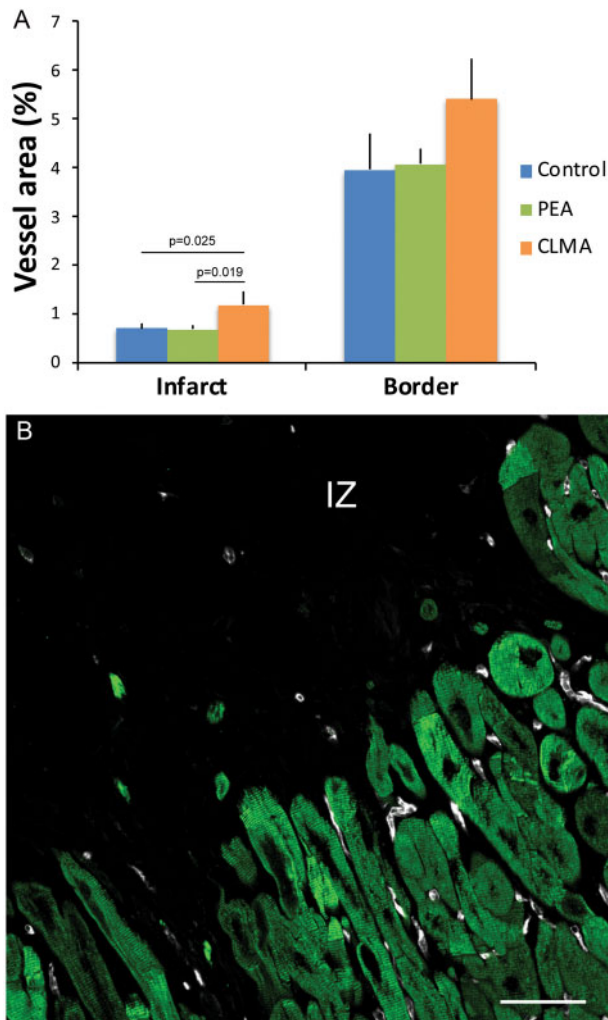
Figure 6: Vascular analysis. (**A**) Vascular density in infarcted and remote zones. Results are presented as the mean percentage of vessel area ± standard deviation. *P*-value <0.05 was considered significantly different. (**B**) Vessels (white) and cardiac troponin I staining (green) in a CLMA-treated animal. IZ and myocardium (green). Scale bar 50 μm. CLMA: cross-linked polycaprolactone; IZ: infarcted zone; PEA: poly(ethyl) acrylate.

CONCLUSION

In summary, we were able to successfully integrate the cardio-patch histologically into damaged myocardium and adjacent to healthy tissue, such that it became an artificial ECM that offered adequate cell niches for the homing of stem cells or exosomes [26]. Results from this study substantially contributed to the generation of an elastomeric cardiopatch and opened the way to create cardiowrap-supported bioprostheses that may become clinically applicable in the supportive treatment of ischaemic heart disease and chronic heart failure [1, 5, 6, 15].

SUPPLEMENTARY MATERIAL

Supplementary material is available at *EJCTS* online.

ACKNOWLEDGEMENTS

The authors acknowledge networking support from the EU COST Action CA16122.

Funding

Conflict of interest: none declared.

REFERENCES

[1] Madonna R, Van Laake LW, Botker HE, Davidson SM, De Caterina R, Engel FB *et al.* ESC Working Group on Cellular Biology of the Heart: position paper for Cardiovascular Research: tissue engineering strategies combined with cell therapies for cardiac repair in ischemic heart disease and heart failure. Cardiovasc Res 2019;115:488–500.

[2] Nielsen SH, Mouton AJ, DeLeon-Pennell KY, Genovese F, Karsdal M, Lindsey ML. Understanding cardiac extracellular matrix remodeling to develop biomarkers of myocardial infarction outcomes. Matrix Biol 2019;75–76:43–57.

[3] Spinale FG, Frangogiannis NG, Hinz B, Holmes JW, Kassiri Z, Lindsey ML. Crossing into the next frontier of cardiac extracellular matrix research. Circ Res 2016;119:1040–5.

[4] Vu DT, Martinez EC, Kofidis T. Myocardial restoration: is it the cell or the architecture or both? Cardiol Res Pract 2012;2012:240497.

[5] Chachques JC, Pradas MM, Bayes-Genis A, Semino C. Creating the bioartificial myocardium for cardiac repair: challenges and clinical targets. Expert Rev Cardiovasc Ther 2013;11:1701–11.

[6] Bayes-Genis A, Galvez-Monton C, Roura S. Cardiac tissue engineering: lost in translation or ready for translation? J Am Coll Cardiol 2016;68: 724–6.

[7] Shafy A, Fink T, Zachar V, Lila N, Carpentier A, Chachques JC. Development of cardiac support bioprostheses for ventricular restoration and myocardial regeneration. Eur J Cardiothorac Surg 2013;43: 1211–19.

[8] Castells-Sala C, Recha-Sancho L, Llucià-Valldeperas A, Soler-Botija C, Bayes-Genis A, Semino CE. Three-dimensional cultures of human subcutaneous adipose tissue-derived progenitor cells based on RAD16-I self-assembling peptide. Tissue Eng Part C Methods 2016;22:113–24.

[9] Martínez-Ramos C, Rodríguez-Pérez E, Garnes MP, Chachques JC, Moratal D, Vallés-Lluch A *et al.* Design and assembly procedures for large-sized biohybrid scaffolds as patches for myocardial infarct. Tissue Eng Part C Methods 2014;20:817–27.

[10] Soler-Botija C, Bagó JR, Llucià-Valldeperas A, Vallés-Lluch A, Castellas-Sala C, Martínez-Ramos C *et al.* Engineered 3D bioimplants using elastomeric scaffold, self-assembling peptide hydrogel, and adipose tissue-derived progenitor cells for cardiac regeneration. Am J Transl Res 2014; 6:291–301.

[11] Biswas M, Sudhakar S, Nanda NC, Buckberg G, Pradhan M, Roomi AU *et al.* Two- and three-dimensional speckle tracking echocardiography: clinical applications and future directions. Echocardiography 2013;30: 88–105.

[12] Dorsey SM, McGarvey JR, Wang H, Nikou A, Arama L, Koomalsingh KJ *et al.* MRI evaluation of injectable hyaluronic acid-based hydrogel therapy to limit ventricular remodeling after myocardial infarction. Biomaterials 2015;69:65–75.

[13] Chachques JC. Cellular cardiac regenerative therapy in which patients? Expert Rev Cardiovasc Ther 2009;7:911–19.

[14] Chachques JC, Marino JP, Lajos P, Zegdi R, D'Attellis N, Fornes P *et al.* Dynamic cardiomyoplasty: clinical follow-up at 12 years. Eur J Cardiothorac Surg 1997;12:560–7.

[15] Varela CE, Fan Y, Roche ET. Optimizing epicardial restraint and reinforcement following myocardial infarction: moving towards localized, biomimetic, and multitherapeutic options. Biomimetics (Basel) 2019;4:7.

[16] Van den Borne SW, Cleutjens JP, Hanemaaijer R, Creemers EE, Smits JF, Daemen MJ *et al.* Increased matrix metalloproteinase-8 and -9 activity in patients with infarct rupture after myocardial infarction. Cardiovasc Pathol 2009;18:37–43.

[17] Ducharme A, Frantz S, Aikawa M, Rabkin E, Lindsey M, Rohde LE *et al*. Targeted deletion of matrix metalloproteinase-9 attenuates left ventricular enlargement and collagen accumulation after experimental myocardial infarction. J Clin Invest 2000;106:55–62.

[18] Sieminski AL, Semino CE, Gong H, Kamm RD. Primary sequence of ionic selfassembling peptide gels affects endothelial cell adhesion and capillary morphogenesis. J Biomed Mater Res Part Res 2008;87:494–504.

[19] Bagó JR, Soler-Botija C, Casaní L, Aguilar E, Alieva M, Rubio N *et al*. Bioluminescence imaging of cardiomyogenic and vascular differentiation of cardiac and subcutaneous adipose tissue-derived progenitor cells in fibrin patches in a myocardium infarct model. Int J Cardiol 2013;169:288–95.

[20] Chachques JC, Trainini JC, Lago N, Cortes-Morichetti M, Schussler O, Carpentier A. Myocardial Assistance by Grafting a New Bioartificial Upgraded Myocardium (MAGNUM trial): clinical feasibility study. Ann Thorac Surg 2008;85:901–8.

[21] Lee H, Ahn S, Bonassar LJ, Kim G. Cell(MC3T3-E1)-printed poly(ϵ-caprolactone)/alginate hybrid scaffolds for tissue regeneration. Macromol Rapid Commun 2013;34:142–9.

[22] Strub M, Van Bellinghen X, Fioretti F, Bornert F, Benkirane-Jessel N, Idoux-Gillet Y *et al*. Maxillary bone regeneration based on nanoreservoirs functionalized ϵ-polycaprolactone biomembranes in a mouse model of jaw bone lesion. Biomed Res Int 2018;2018:7380389.

[23] Rohman G, Huot S, Vilas-Boas M, Radu-Bostan G, Castner DG, Migonney V. The grafting of a thin layer of poly(sodium styrene sulfonate) onto poly(ϵ-caprolactone) surface can enhance fibroblast behavior. J Mater Sci Mater Med 2015;26:5539.

[24] Spadaccio C, Nappi F, De Marco F, Sedati P, Taffon C, Nenna A *et al*. Implantation of a Poly-L-Lactide GCSF-Functionalized Scaffold in a model of chronic myocardial infarction. J Cardiovasc Trans Res 2017;10: 47–65.

[25] Monnet E, Chachques JC. Animal models of heart failure: what is new? Ann Thorac Surg 2005;79:1445–53.

[26] Bellin G, Gardin C, Ferroni L, Chachques JC, Rogante M, Mitrecic D *et al*. Exosome in cardiovascular diseases: a complex world full of hope. Cells 2019;8:166.

Exosome in Cardiovascular Diseases: A Complex World Full of Hope

Gloria Bellin [1,2] **, Chiara Gardin** [1,2]**, Letizia Ferroni** [1,2]**, Juan Carlos Chachques** [3]**, Massimo Rogante** [4] **, Dinko Mitrečić** [5]**, Roberto Ferrari** [6] **and Barbara Zavan** [1,6,*]

[1] Department of Biomedical Sciences, University of Padova, 35131 Padua, Italy; gloria.bellin@gmail.com (G.B.); chiara.gardin@unipd.it (C.G.); letizia.ferroni@unipd.it (L.F.)
[2] Maria Pia Hospital, GVM Care & Research, 10132 Torino, Italy
[3] Laboratory of Biosurgical Research (Alain Carpentier Foundation), Pompidu Hospital, University Paris Descartes, 75015 Paris, France; j.chachques-ext@aphp.fr
[4] Rogante Engineering Office, 62012 Civitanova Marche, Italy; main@roganteengineering.it
[5] Laboratory for Stem Cells, Croatian Institute for Brain Research, University of Zagreb School of Medicine, 10000 Zagreb, Croatia; dinko.mitrecic@mef.hr
[6] Maria Cecilia Hospital, GVM Care & Research, 48033 Ravenna, Italy; fri@unife.it
* Correspondence: barbara.zavan@unipd.it; Tel.: +39-049-827-6096

Abstract: Exosomes are a subgroup of extracellular vesicles containing a huge number of bioactive molecules. They represent an important means of cell communication, mostly between different cell populations, with the purpose of maintaining tissue homeostasis and coordinating the adaptive response to stress. This type of intercellular communication is important in the cardiovascular field, mainly due to the fact that the heart is a complex multicellular system. Given the growing interest in the role of exosomes in cardiovascular diseases and the numerous studies published in the last few decades, we focused on the most relevant results about exosomes in the cardiovascular filed starting from their characterization, passing through the study of their function, and ending with perspectives for their use in cardiovascular therapies.

Keywords: exosomes; extracellular vesicle; cardiovascular disease

1. Introduction

Exosomes (EXOs) are a subgroup of extracellular vesicles (EVs), ranging in size from 30 to 100 nm, released by different cell types [1]. To date, they were found in numerous body fluids such as plasma, serum, saliva, amniotic fluid, breast milk, and urine; moreover, they are also released in cell culture media [2]. EXOs are rich in bioactive molecules, including DNA, messenger RNAs (mRNAs), microRNAs (miRNAs), and proteins; moreover, by transferring their bioactive cargos, they are important drivers in intercellular communication.

Many studies focused on the complex mechanisms of EXO biogenesis, secretion, and cargo loading; in fact, several steps are needed from the formation of intraluminal vesicles until fusion with the plasma membrane, passing through the loading of cargos. EXOs generate from the invagination of endosomes which form multivesicular bodies (MVBs) and they are secreted through the fusion of MVBs with the cell membrane; this process is mediated by the Rab family of proteins [3]. EXO composition is dependent on the cell type of origin, and is largely reflective of its physiological or pathological state. This means that the secretion, content, and function of EXOs strongly vary in response to changes in the cell microenvironment [4]. The precise selection of EXO cargo is not yet well clarified, although it seems that the protein sorting into EXOs is principally managed by

endosomal sorting complexes required for transport (ESCRT) or by sphingolipids (ESCRT-dependent or ESCRT-independent pathways) [5,6]. Observations about RNA species suggested that some RNAs present motifs that may represent elements that favor their loading into EXOs [7] (Figure 1). Protected from the EXO lipid bilayer, protein and RNA cargo can persist in the extracellular space without undergoing degradation. Once secreted, EXOs can enter neighboring target cells or travel into the body fluids to even reach cells in distant districts; it was demonstrated that target cells internalize EXOs through a variety of methods such as endocytosis, membrane fusion, or ligand receptor binding, depending on source cells, target cells, and environments [8,9].
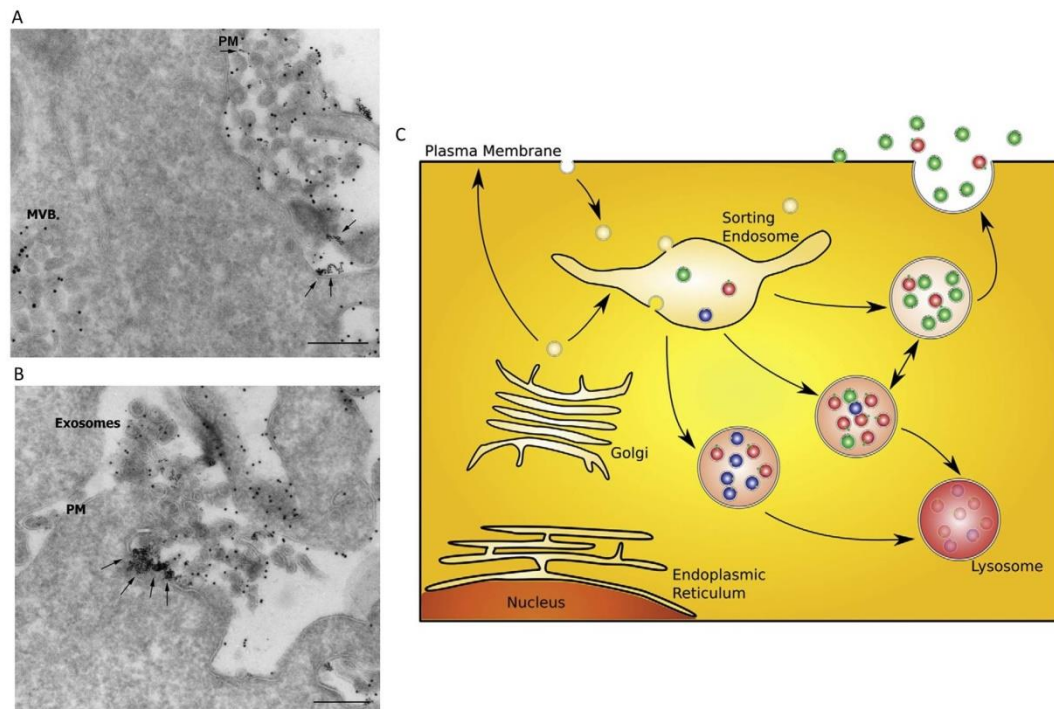

Figure 1. Release of exosomes (EXOs) and a sorting model. (**A**,**B**) Release of EXOs upon exocytic fusion of multivesicular bodies (MVBs) with the plasma membrane; arrows indicate the fusion profile. PM: plasma membrane; MVB: multivesicular body. Scale bars: 200 nm. (**C**) A proposed model for sorting of cargo into different MVB subpopulations. Different hypothetical MVB subclasses with distinct populations of intraluminal vesicles (red, green, and blue) are shown. Whether the MVBs contain a mixture of different intraluminal vesicles as depicted in the figure is not known. Sorting of cargo may already start within the biosynthetic pathway, at the plasma membrane, or within an endosomal compartment. Modified from Reference [1].

This evidence leads EXOs to become an attractive focus in biomedical research for investigating their role in different physiological and pathological settings as signaling mediators, biomarkers, and potential therapeutic targets.

Recently, EXOs earned interest in the cardiovascular field due to the fact that, in a multicellular system, such as the heart, communication between different and not always close cells plays a fundamental role in the maintenance of physiological cardiac homeostasis and in the adaptive response to stress; EXOs are suitable candidates to have a central role in intercellular exchanges of information. It was demonstrated that they are involved in a wide range of cardiovascular processes, both physiological and pathological, with beneficial or detrimental activity [10–13].

EXOs are released practically from all cells in the cardiovascular system and it was shown that stress conditions such as hypoxia or inflammation modulated their cargos and their release in conjunction with the target cells, contributing to improving or to impairing heart function [14] (Figure 2). Furthermore, Waldenström and colleagues highlighted the heterogeneity of microvescicles

(MVs) and EXOs from the same cell type; in cardiomyocytes (CMs), 80% of the vesicles from the main cell population resulted positive for flotillin-1 surface antigen, while 30% were positive for carveolin-3, a protein exclusively present in cardiac muscle cells [15]. A part of them displayed an electron-dense appearance and another part displayed an electron-lucent interior. They hypothesized that these differences could imply a difference also in their cargo and target cells [15] (Figure 2).
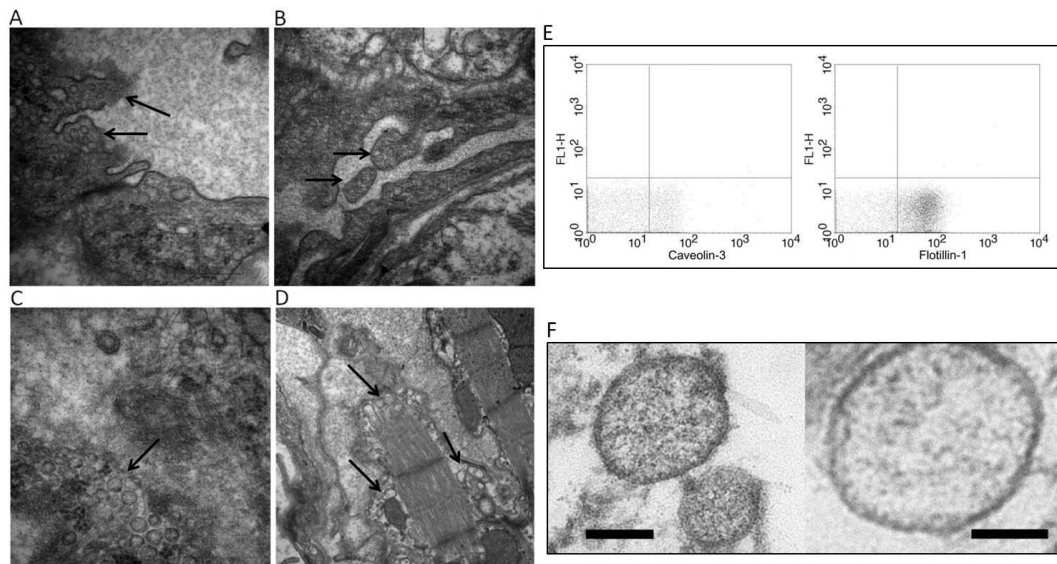

Figure 2. Electron microscopy of heart tissue. (**A**,**B**) Budding of the vessel wall to release the exosomes into the lumen (black arrows); (**C**) exosomes in the extracellular space; (**D**) exosomes released by myocyte fiber. Modified from Reference [16]. (**E**) Detection of proteins on cardiomyocyte (CM) EXO surface with flow cytometry. Mouse anti-caveolin-3 was detected on approximately 30% of EXOs (left), while mouse anti-flotillin-1 was detected on approximately 80% of EXOs. The distribution of EXOs presenting caveolin-3 and flotillin-1 indicates that the sample contains more than one population of EXOs. (**F**) Transmission electron microscopy of purified CM microvesicles (MVs)/EXOs. On the left, MVs/EXOs that display an electron-dense appearance are shown; on the right, MVs/EXOs that display an electron-lucent appearance are shown. Scale bar: 100 nm. Modified from Reference [15].

The multitude of cardiovascular processes in which EXOs are involved affords them great potential in the diagnostic and therapeutic fields as a novel alternative to whole-cell therapies. This is because they are more stable than cells, as well as being biocompatible and non-immunogenic; moreover, they are resistant to cryo-conservation without degrading [17]. However, it is necessary to say that EXO collection, isolation, and purification processes are still undergoing standardization. In fact, as highlighted by Tang and colleagues, different isolation methods lead to a discrepancy in purity, size, and concentration of EXOs and their cargo [18]. It follows that the populations of vesicles isolated with different methods are not homogeneous, and probably contain more than just exosomes. The lack of standardized methods can explain the difficulties in reproducibility and the discrepancies of results of some studies.

In this review, we summarize the findings about the role of EXOs in the cross-talk between the different cardiac cell populations and their potential as diagnostic biomarkers and therapeutic means in cardiovascular diseases.

2. Exosomes from Different Cardiac Cells, Their Content, and Their Ability to Modulate Cell Behavior

A large part of heart volume is built by cardiac muscle, while the most abundant non-myocyte cell type is represented by cardiac fibroblasts (CFs) that account for about 90% of non-muscle cells. In contact with these cells, there are endothelial cells (ECs) that have important roles in cardiac

homeostasis. Moreover, several studies highlighted the presence of resident cardiac-derived progenitor cells (CPCs) that are involved in the post-injury response [19,20]. The presence of such cells in the heart suggests the importance of heterocellular communication and the necessity to investigate the way in which this communication takes place. In this sense, EXOs are the main candidate for mediation between the various cell populations.

2.1. Cardiomyocytes

The first evidence that CMs release EXOs was provided by Gupta et al., who showed that EXOs were released both in physiological conditions and after hypoxia, with an increase in their release and in their content of heat-shock protein 60 (HSP60) under stress conditions [14]. A further study demonstrated that HSP60s contained in EXOs were bound to the membrane and were not released, preventing the pro-apoptotic effects induced by circulating HSP60 [10]. In the same study, proteomic analysis revealed that EXOs from primary CMs contained a pool of proteins that were common, but differed in amount, in EXOs obtained from CMs which underwent ethanol or hypoxia/reoxygenation stimuli. This pool included HSP60, tropomyosin-α, glyceraldehyde 3-phosphate dehydrogenase (GAPDH), myomesin, myosin-binding protein C, α-Cristallin B chain, and valosin-containing protein (VCP), while HSP27 and HSP90 were found only in hypoxia/reoxygenation-derived EXOs [10]. Moreover, EXOs from CMs that underwent hypoxia treatment seemed to promote apoptosis in nearby CMs due to the presence of tumor necrosis factor-α (TNF-α) in their cargo, favored by the activation of hypoxia-inducible factor-1α (HIF-1α) [12]. Another study demonstrated that hypoxic condition enriched EXOs in miRNA-30a that was efficiently transferred between CMs, favoring the maintenance of autophagic response probably through targeting *beclin-1* and the *Atg12* gene. Furthermore, CM transfection with a miRNA-30a inhibitor or a block of EXO release from CMs attenuated hypoxia-induced apoptosis [21]. Other miRNAs present in CM EXOs after hypoxia were found to be involved in the modulation of the apoptotic pathway; Zhang and colleagues indicated that rno-miR-21-5p, rno-miR-378-3p, rno-miR-152-3p, and let-7i-5p were upregulated after 48 h of hypoxia and, in particular, rno-miR-21-5p and rno-miR-378-3p appeared to have anti-apoptotic effects [11].

Since cardiovascular impairment is a major complication of diabetes, several studies focused on the involvement of EXOs in heart failure in diabetic conditions. For diabetic patients, physical exercise is important to decrease the possibility of developing cardiac dysfunction. Chaturvedi and colleagues studied EXOs released from cardiac muscle during exercise. They discovered that so-stimulated CM EXOs contained an elevated amount of mmu-mir-29b and mmu-mir-455, and that these miRNAs prevented the activation of matrix metalloproteinase 9 (MMP9), preserving the heart from the development of fibrosis and myocyte uncoupling [16]. This evidence served as a starting point to explore CM EXOs as a therapy for cardiac remodeling, since MMP9 inhibitors were not successful [16].

It was proven that EXOs from CMs could be internalized from other cells such as CFs and ECs, promoting the modulation of receiving cell behaviors. For example, the presence of CM EXO DNA in the CF cytosol and nucleus was shown, and this promoted gene expression modification. In particular, 175 genes were upregulated and 158 were downregulated in fibroblasts treated with CM EXOs [15]. A recent study indicated that the interaction between CMs and CFs is important in the progression of chronic heart failure, promoting the development of cardiac hypertrophy and dysfunction [22]. High expression of hsa-miR-217 in pathological rat CMs seemed to favor its release through EXOs that are taken up by CFs, promoting their proliferation and activation, and leading to heart fibrosis [22].

The close anatomical and functional relationship between CMs and ECs implicates the ability of CMs to communicate also with ECs and vice versa, above all during stress and pathological conditions. Wang et al. investigated the role of EXOs in CM and EC cross-talk in diabetic rats, showing that EXOs from pathological CMs were rich in rno-miR-320 and poor in rno-miR-126. This cargo modulated *insulin-like growth factor-1 (IGF-1)*, *HSP20*, and *Ets2* expression in ECs, promoting the downregulation of these genes; this seemed to lead to an inhibition of EC proliferation, migration, and tube-like

formation [23]. On the contrary, deprivation of glucose, another stress condition, enhanced the release of EXOs from CMs with a glucose-dependent regulation of the cargo; CMs in normal culture conditions were shown to release EXOs that contained proteins mainly related to cell structure, growth, and survival, as well as mmu-miR-17, 20a, 23b, 30b, and 132. Contrariwise, CMs deprived of glucose produced EXOs rich in proteins involved in cell metabolism and in the proenergetic pathway, as well as mmu-miR-16, 17, 19a, 19b, 21, 23a, 23b, 30c, 125b-5p, 126-3p, 301a, and 301b [24] (Figure 3).
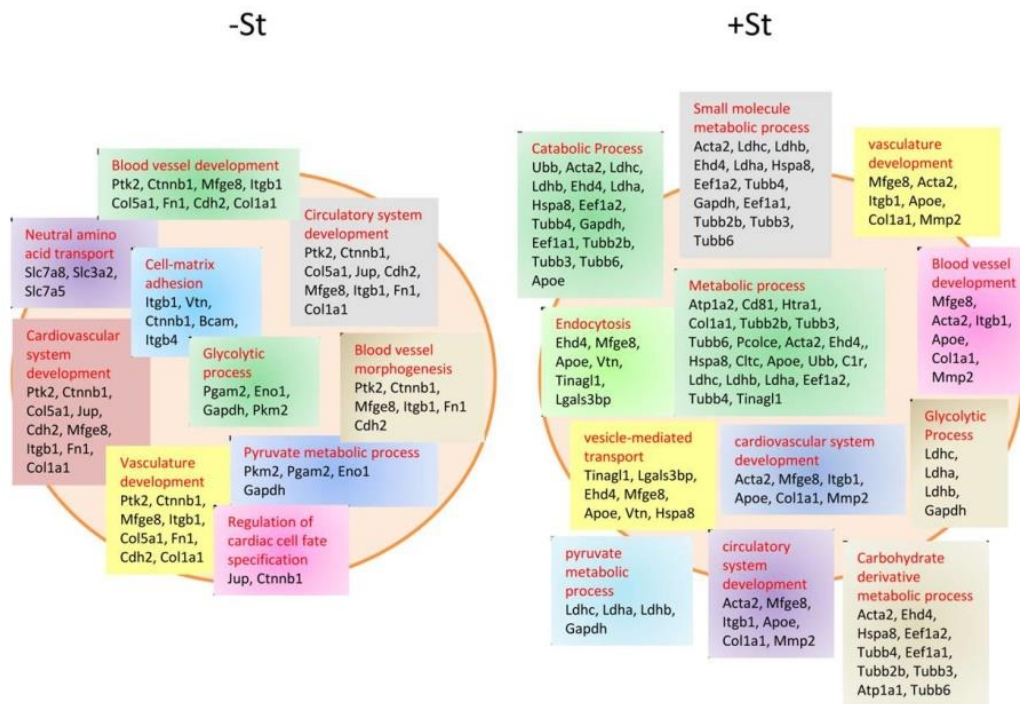

Figure 3. Schematic representation of protein content in EXOs from starved (+St), i.e., glucose-deprived, and non-starved (−St) CMs. CMs deprived of glucose change the protein pool contained in their EXOs, promoting their loading with proteins related to metabolic and catabolic processes, as well as blood vessel and cardiovascular development [24].

In particular, mmu-miR-17, 19a, 19b, 20a, 30c, and 126 were correlated with an increase in angiogenesis when internalized by ECs. This was demonstrated by Garcia et al., who showed a great propensity of EC cells to enter the synthesis (S) phase, and to increase tube formation when treated with starved-CM EXOs [24].

2.2. Cardiac Fibroblasts

CFs are the main cells involved in extracellular matrix (ECM) turnover, and, due to their secretory activity, they influence the physiology of other cells in the heart [25]. Despite this, only few works investigated CF EXO composition and activities. One was performed by Cosme and colleagues, who mapped and compared the proteomic profile of whole-CF lysate, CF secretome, and CF EXO content in normoxic and hypoxic conditions (Figure 4).

Focusing on EXOs, they found that normoxic and hypoxic conditions modified the number and the content of CF EXO proteins; under normoxic conditions, they identified 1752 proteins, while, following hypoxia, there were 1616 proteins. Moreover, comparing normoxia vs. hypoxia, 144 proteins resulted differentially expressed. Hypoxic conditions promoted EXO enrichment in ECM proteins such as multiple collagen type, perlecan, and fibronectin. Furthermore, they found an overrepresentation of mitochondria-associated proteins, and hypothesized that EXOs could be used by cells to remove dysfunctional mitochondria during stress conditions [25].
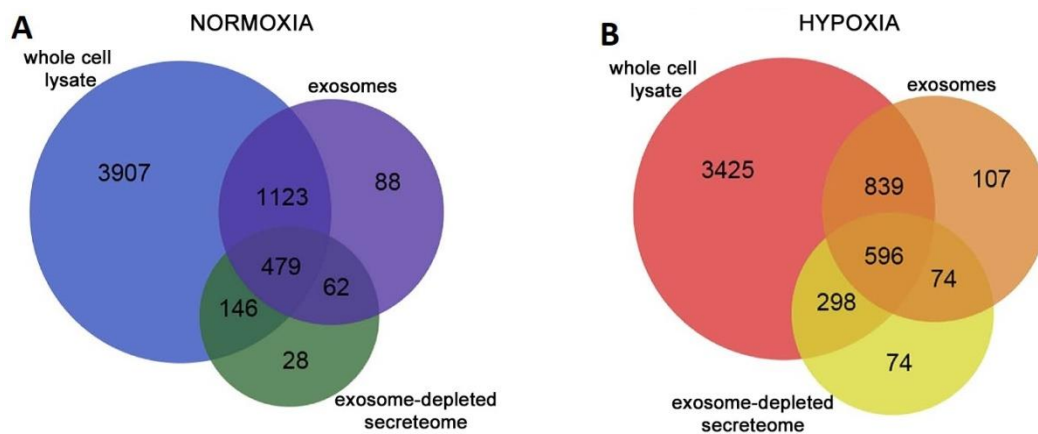
Figure 4. Summary of proteomics data acquired using a multidimensional protein identification technology approach. Venn diagrams representing the overlap of protein identifications between cardiac fibroblast (CF) whole-cell lysate, exosome, and secretome collected in (**A**) normoxic conditions and (**B**) hypoxic conditions. The number of proteins contained in the three fractions changed depending on the culture conditions. Modified from Reference [25].

They also demonstrated that, depending on the time of co-treatment, CF EXOs had different effects on CM viability; if CF EXOs were added to CMs immediately before CM hypoxia treatment, they improved CMs viability; contrariwise, they reduced CM viability if added before the CM reoxygenation phase.

In addition to proteins, CF EXOs also contain miRNAs. It was shown that the 25.5% of fibroblast EXO miRNAs were represented by star miRNAs and, interestingly, Bang et al. discovered that fibroblasts were rich in rno-miR-21, while fibroblast-derived EXOs were enriched with rno-miR-21*. From their study, it seemed that rno-miR-21* was transported from CFs to CMs via EXOs, and that it could be involved in CM hypertrophy [26]. Tian and colleagues demonstrated that treatment with TNF-α favored the enrichment of CF EXOs with rno-miRNA-27a, rno-miRNA-28a, and rno-miRNA-34a. These miRNAs were transferred to CMs promoting the expression of hypertrophic markers such as atrial natriuretic peptide and β-myosin heavy chain in CMs [13].

The use of EXOs by CFs to communicate with CMs was also investigated by Lyu and colleagues, who noted that angiotensin II (AngII)-treated CFs stimulated the release of EXOs that were taken up by CMs. These EXOs in turn upregulated AngII expression together with the expression of its receptors in CMs, enhancing AngII-related cardiac hypertrophy [27].

From these studies, we can deduce that CFs utilize EXOs to communicate predominantly with CMs.

2.3. Endothelial Cells

Heart microvasculature is fundamental for cardiac health and cardiac tissue homeostasis. ECs, which form the endothelial barrier between blood and surrounding tissues, have a primary role in the maintenance of this homeostasis, especially following stress signals such as inflammation or hypoxia. The response of ECs to stress or damage signals leads not only to a release of growth factors and cytokines, but also EXOs that mediate their communication with each other and with the other cardiac compartments.

A study carried out in 2012 showed that ECs cultured under different conditions released EXOs whose contents reflected cellular stress, varying in relation to the received stimuli [28]. Quantitative proteomics and mRNA arrays revealed that EXOs from ECs that underwent hypoxia or inflammation clearly differed from control EC EXOs; if stimulated with hypoxia, they presented a higher content of proteins involved in ECM remodeling, such as fibronectin and collagen, and an enrichment in mRNAs linked to stress response and apoptosis genes; if treated with TNF-α to mimic inflammation, EXOs

resulted enriched in several factors concerning superoxide protection, immune response, and nuclear factor κB (NF-κB) pathway [28].

EXOs are used by ECs to communicate with each other and, particularly, to manage angiogenesis. It was found that delta-like 4 factor (Dll-4), an important factor that regulates angiogenesis, was present into EXOs released from ECs overexpressing Dll-4, and that these EXOs were taken up by the neighboring ECs. The transfer of these EXOs through ECs promoted the increase in angiogenesis by inhibiting Notch signaling, without requiring cell–cell contact [29]. Another factor delivered by EC EXOs, which resulted implicated in the modulation of angiogenesis and vessel formation, is hsa-miR-214 [30]. Van Balkom and colleagues showed the transfer of this miRNA between ECs and demonstrated that this caused the downregulation of ataxia telangiectasia mutated (ATM) in recipient cells. ATM is responsible for the prevention of cell-cycle progression; thus, its downregulation means a repression of cell senescence and an induction of the angiogenetic program [30].

In particular conditions such as peripartum cardiomyopathy, ECs, stimulated by 16-kDa N-terminal prolactin fragment (16K PRL), overexpress miRNA-146a that exerts anti-angiogenic and anti-proliferative effects on ECs. This miRNA is also secreted through EXOs release by ECs that are efficiently taken up by CMs, thus modulating their activity [31]. Halkein et al. demonstrated that EC EXOs, enriched in miR-146a, taken up by CMs, promoted the decrease of CM metabolic activity and downregulated Erbb4, Notch1, and Interleukin-1 receptor associated kinase 1 (Irak1) expression, proteins which are normally upregulated in the maternal heart, leading to the development of peripartum cardiomyopathy [31].

2.4. Cardiac-Derived Progenitor Cells and Cardiosphere-Derived Cells

Several studies demonstrated that the adult heart contains a group of heterologous cells, senescent in physiological conditions, capable of being activated by injuries and of differentiating into new myocytes or vascular cells; these cells are named cardiac-derived progenitor cells (CPCs) [32,33]. These cells spontaneously diffuse out from ex vivo cultures of heart tissue. When cultured in suspension, CPCs have the tendency to form spherical aggregates, denominated cardiospheres (CDCs). These aggregates differ from CPCs and present different properties [20].

It was shown that EVs can be released from CPCs and CDCs, and it was shown that EXOs were the predominant fraction of EVs [34,35]. In 2014, Barile et al. studied the effects of conditioned medium from CPCs, which contained EXOs, on the HL-1 cardiomyocytic cell line and on human umbilical vein endothelial cells (HUVEC), finding that it decreased HL-1 cell apoptosis and promoted tube formation in the HUVEC culture. MicroRNA transcriptional profiling of EV content underlined an enrichment in hsa-miR-210, hsa-miR-132, hsa-miR-146a-3p, and hsa-miR-181, compared with the profiling of fibroblasts EVs [36]. In particular, Barile and colleagues hypothesized that the presence of a high amount of hsa-miR-210 sustained the anti-apoptotic effect, as it is associated with the downregulation of its targets ephrin A3 and Protein-tyrosine-phosphatase 1 (PTP1), while the increased presence of hsa-miR-132, associated with the functional downregulation of its target RasGap-p120, was indicated as responsible for the angiogenetic effects [36]. The protection of CMs from apoptosis by CPC EXOs could be sustained also by the content of mmu-miR-21, which seemed to downregulate programmed cell death 4 (PDCD4) expression; indeed, this factor is involved in the miRNA-21/PDCD4 axis that importantly mediates CM apoptosis induced by oxidative stress [37].

A recent study suggested that the cardioprotective capacity of CPCEXOs could be due also to the presence of pregnancy-associated plasma protein-A (PAPP-A) on their surface [38]. The active form of this protein cleaved Insulin-like growth factor binding protein-4 (IGFBP-4) promoting the release of Insulin-like growth factor-1 (IGF-1), a key cardioprotective factor. Moreover, EXOs from CPCs favored the phosphorylation of Insulin-like growth factor receptor (IGFR) and intracellular Extracellular-signal regulated kinase 1 and 2 (Erk1/2) in CMs treated with staurosporine [38].

Regarding CDCs, Ibrahim and colleagues also showed that EXOs derived from them had cardioprotective function. They resulted enriched in hsa-miR-146 compared to those of the

fibroblasts [39]; this miRNA has known targets Irak1 and Traf6, two signaling mediators of the Toll-like receptor (TLR)–NF-κB axis [40,41]. In this study, the exposure of CMs to an miR-146a mimic promoted their protection against oxidative stress and, as a consequence, CM viability increased. Furthermore, the knockout of miR-146a in mice (146a KO) significantly impaired heart function after myocardial infarction (MI), also causing adverse tissue remodeling compared to wild-type (WT) mice or miR-146a KO mice injected with an miR-146a mimic (146a KO-R) [39] (Figure 5). The authors concluded that this evidence pointed to miRNA-146a potentially mediating the benefits of CDC EXOs.
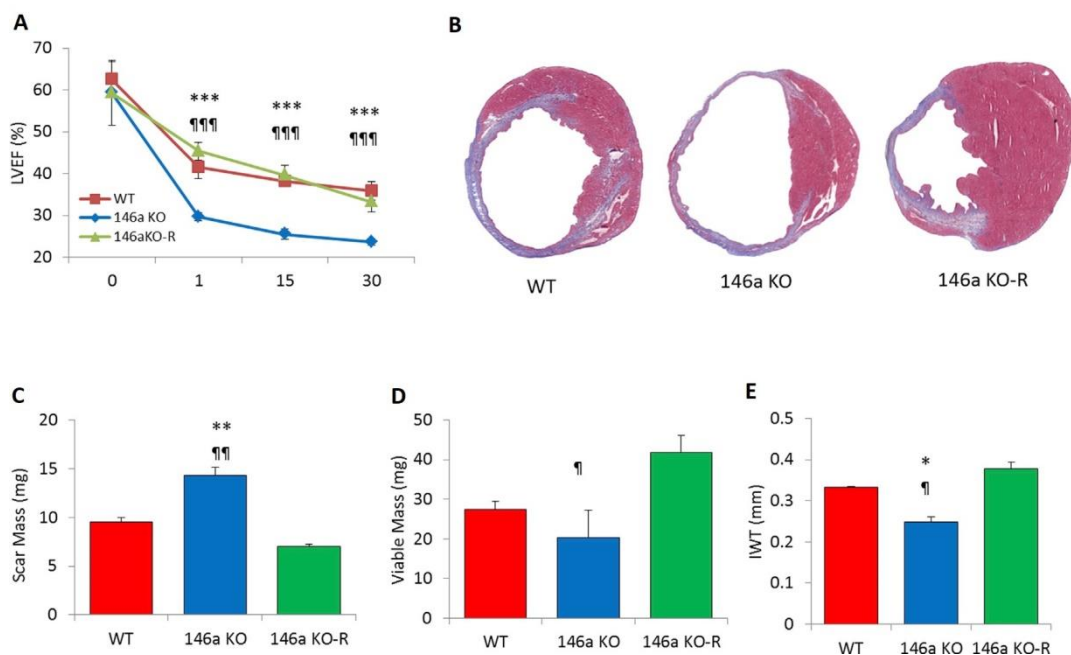

Figure 5. Involvement of microRNA (miR)-146a in the impairment of heart function after myocardial infarction (MI). (**A**) Measurement of left-ventricular ejection fraction indicates that 146a knockout (KO) animals have severely impaired cardiac function and structure following acute MI compared to wild-type (WT) or 146a KO-R mice. (**B**) Representative Masson's trichrome-stained sections of hearts from three groups show the different tissue regeneration after MI. (**C–E**) Morphometric analysis reveals impairment of cardiosphere (CDC)-mediated benefits as evident in pooled data for scar mass, viable mass, and infarct wall thickness (IWT) in hearts of 146a KO mice. * $p < 0.05$, ¶ $p < 0.05$; ** $p < 0.01$, and ¶¶ $p < 0.01$, *** $p < 0.001$, and ¶¶¶ $p < 0.001$ using Student's *t*-test (* KO versus WT; ¶ KO versus KO-R). Data are represented as means and standard errors of the mean (SEM). Modified from Reference [39].

Most of the studies that investigated the role of CPC EXOs on different populations of infarcted heart cells did not take in consideration that, in physiological conditions, CPCs are also exposed to hypoxic conditions. In their work, Gray et al. paid attention to this and utilized EXOs from CPCs exposed to 3 h or 12 h of hypoxia in treated ECs and CFs. They pointed out that 12-h hypoxic CPC EXOs significantly enhanced tube formation in ECs and decreased pro-fibrotic factor expression in CFs, while 3-h hypoxic CPC EXOs or normoxic CPC EXOs did not have such pronounced effects [42]. Interestingly they saw that hypoxic EXOs were poor in miRNA-320, miRNA-222, and miRNA-185 content, correlated with anti-angiogenic, pro-apoptotic and anti-migration, and pro-fibrotic effects, respectively [42].

At the beginning of 2018, Nie et al. published a paper in which they performed proteomic and RNA sequencing analysis of the CPC secretome [43]. The results were in agreement with previous studies and confirmed the pro-survival, pro-angiogenic, and pro-mitogenic effects of CPC EXOs content. They found elevated levels of miRNA precursors and miRNAs that stimulate cell survival, proliferation, and angiogenesis, such as hsa-miR-3615, hsa-miR-6087, hsa-miR-1244, and hsa-miR-3687,

and, in addition to these, small and long non-coding RNAs. Interestingly, proteomic analysis revealed that, within the EVs, 93% of proteins had their corresponding mRNA, suggesting that they were captured during the translation process. Consequently, proteins also resulted to be implicated in cell survival, proliferation, and angiogenesis [43].

3. Exosomes as Biomarkers in Cardiovascular Diseases

In addition to being internalized by neighboring cells, EXOs produced by cardiac cells are released into the body fluids. This allows exploiting EXOs as biomarkers that indicate a pathological state, considering that EXO content could vary in relation to it.

MicroRNAs are the most studied elements contained in EXOs for their role as new biomarkers in cardiovascular diseases. The majority of miRNAs isolated from plasma contained EXOs and bound to RNA-binding proteins, while only few miRNAs were free [44]; through analyzing the content of circulating EXOs, it was and it will possible to identify miRNAs that, changing in quantity, can be considered as biomarkers.

Focusing on cardiovascular diseases, different miRNAs were individualized for this purpose; for example, hsa-miR-1 and hsa-miR-133a, two cardiac-specific miRNAs, were demonstrated to be upregulated in serum from patients with acute coronary syndrome (ACS), and they were very likely stored in EXOs [45].

In acute pathologies, such as ACS and acute myocardial infarction (AMI), it is very important to rapidly individualize them. The classical biomarkers used to diagnose AMI are troponin and creatinine kinase MB, which sometimes coordinate with other biomarkers. Troponin levels peak at 12 h from the onset of cardiac damage, and their levels are proportional to the infarct size [46]. Recently, circulating miRNAs were discovered that were upregulated in the plasma of AMI patients, which reached their peak level earlier then troponin. An example was hsa-miR-208a; it was undetectable in healthy patients, but clearly appeared in 100% of AMI patients after 4 h from the onset of chest pain, very early compared to the appearance of detectable traces of troponin [47]. From the same family, hsa-miR-208b was also evaluated as an AMI biomarker. It was found that this miRNA was significantly increased in AMI patients within 12 h, making it a potentially good biomarker, but not one superior to troponin as they have a similar trend. The same consideration was made for hsa-miR-1, hsa-miR-133a, and hsa-miR-499 [48]. A research by Gidlöf et al. showed that the upregulation of plasma levels of hsa-miR-208b and hsa-miR-499-5p corresponded to an increase in the risk of death or heart failure, giving an indication of the prognosis [49]. Matsumoto and colleagues found that three particular p53-responsive miRNAs enriched in circulating EXOs, hsa-miR-192, hsa-miR-194 and hsa-miR-34a, were upregulated in the serum of AMI patients that experienced development of heart failure within one year, leading them to be considered as possible prognostic markers [50].

Few studies analyzed the proteomic profile of EXOs found in the bloodstream of MI patients. Cheow et al. identified six novel proteins that might be biomarkers of myocardial injury; these belonged to complement activation (C1Q1A and C5), lipid metabolism (APOD and APOC3), and platelet activation pathways (GP1BA and PPBP) [51].

Altogether, the studies reported above indicated that the heart releases characteristic EXOs following the onset of injury. The content of these EXOs might be useful for an early diagnosis and for hypothesizing, and thereby trying to prevent, a future prognosis. Some elements seem to be able to help formulate a diagnosis earlier than those actually used, while others, added to the classical analysis, could serve to pronounce a more precise diagnosis.

4. Exosomes as Therapeutic Agents in Cardiovascular Diseases

The possible use of EXOs as a substitute to whole-cell therapy received great interest. EXOs, in fact, possess several advantages compared to cells for therapeutic use; they are biocompatible, non-immunogenic, and non-tumorigenic; moreover, they are physiologically more stable than cells, can circulate all over the body, and are able to cross blood–brain barrier (BBB). Moreover, they are

suitable to be loaded with therapeutic cargos, and they are more resistant to freezing and thawing procedures than cells, favoring long-term storage [17].

As reviewed before, several studies were conducted to understand EXO function in cardiovascular physiology and pathology. Through these researches, it emerged that EXOs generated from different cardiac cell types in different conditions could contain cargo that generates positive or negative effects on target cells. This gave some ideas on how to exploit EXOs for therapeutic approaches, which can be divided into two big categories: those that counteract adverse functions of harmful EXOs, and those that take advantage of and enhance the cardioprotective effects of beneficial EXOs.

4.1. Strategies to Attenuate Adverse Effects of Exosomes

As already mentioned, it was discovered that some factors contained in EXOs generated in pathological conditions have a detrimental role in cardiovascular diseases.

Studies on EXO biogenesis and trafficking gave suggestions on how to attenuate EXO adverse effects during diseases, starting from their formation and ending with their release and uptake from target cells.

To block EXO formation, it was found efficient to inhibit ceramide formation using inhibitors of neutral sphingomyelinases, such as GW4869, [6], or using amiloride, an anti-hypertensive drug that blocks Ca^{2+}-dependent MVB formation [52]. Another way seemed to be the inhibition of the interaction between syndecan proteoglycans and its cytoplasmic adaptor syntetin, which interacts with programmed cell death-6-interacting protein (PDCD6IP or ALIX), an important protein involved in EXO biogenesis [53].

Regarding EXO release and uptake from target cells, the various mechanisms through which they occur are not yet detailed, and the fact that they differ through cell types makes them a difficult target to approach. Moreover, most studies were performed on tumor cells that represent a very particular condition, making them difficult to transfer to the cardiovascular field.

All these pathways offer many opportunities to look for right ways to inhibit harmful EXOs; however, at the same time, interfering with these processes, fundamental also for the regulation and the maintenance of physiological state, could be dangerous because of off-target effects.

4.2. Strategies to Exploit Exosomes in Cardiovascular Therapy

In the last few years, stem-cell therapies caught attention in many research fields, and were found to be successful in many cases. However, in the cardiovascular field, they did not appear so promising; they displayed poor engraftment and survival, as well as the occurrence of arrhythmias and immune rejection after transplantation [54].

Increasing evidence demonstrated that several cell types, above all stem cells, display their paracrine effects through EXO release. This shifted the focus from cell therapy to cell-free therapy approaches, and stem cells represent the most promising EXO source for cardiovascular therapy.

For investigating cardioprotective and cardiac repair effects of EXOs, scientists isolated them from stem cells of different origin: mesenchymal stem cells (MSCs), induced-pluripotent stem cells (iPSCs), and CPCs. Arslan et al. were among the first to investigate the role of MSC EXOs on myocardial ischemia/reperfusion injury, finding that EXO treatment activated pro-survival signaling by increasing ATP and Nicotinamide adenine dinucleotide (NADH) levels, and decreasing oxidative stress. Moreover, cardiac function was enhanced and infarct size was reduced [55]. Feng and colleagues showed that MSCs that underwent ischemic preconditions produced EXOs able to improve cardiac function after MI, by reducing infarct size and fibrosis [56]. Another work explained that EXOs derived from MSCs overexpressing GATA-4 resulted enriched in rno-miR-19a, which could be the promoter of increased CM survival in a hypoxic environment [57].

As already mentioned, EXOs from CPCs also resulted having regenerative potential after myocardial infarction. Several works demonstrated that they reduce CMs apoptosis, increase tube formation, and decrease the development of fibrosis. This leads to an improvement in cardiac

function [36,39,42]. Interestingly, the pretreatment of CPCs with MSC EXOs seems to modify CPC EXO cargo so as to increase in rno-miR-147 and rno-miR-503-3p levels, and decrease in rno-miR-207, rno-miR-326-5p, and rno-miR-702-5p levels. These cells, once injected, were shown to promote an increase in vessel density at the infarct site and to ameliorate cardiac function [58]. When stimulated with embryonic system-cell (ES) EXOs, CPCs express more CM and EC genes. The injection of pre-stimulated CPCs resulted in increased cardiac function and reduced infarct size, while the direct injection of ES MVs/EXOs increased vessel density and improved cardiac function [59].

These studies suggest that changing donor cell conditions is a valid way of modifying EXO content, potentiating their cardiovascular protection ability. In addition, pretreatment of stem cells with EXOs derived from other cells can enhance their therapeutic effects.

A curious and unusual study was performed by Middleton and colleagues, who took a cue from newts, as they can regenerate lost organs and tissues, including the heart, and analyzed the compatibility of newt EVs with mammalian cells [60]. They extracted EVs form newt myogenic precursor cells (A1) and, after seeing that, in many ways (size, morphology, content, surface agents, and GW4869 sensitivity), they were similar to mammalian ones, they treated mammalian CMs with these vesicles. Gene expression analysis indicated that treated CMs were more resistant to oxidative stress and, thus, had enhanced cell survival, due to the activation of the Protein kinase B (AKT) pathway [60]. This evidence makes A1 EXOs and their content interesting candidates for therapeutic studies in cardiovascular fields.

In addition to the natural effect of stem-cell EXOs, methodologies for loading non-native cargo continue to be investigated to extend their therapeutic potential (Figure 6). Currently, three main strategies are available: endogenous encapsulation, and passive or active exogenous cargo encapsulation. Endogenous loading plans to modify parent cells via transfection or specific treatments, whereby derived EXOs will reflect the change in parent cells, and part of them will contain the loaded elements [61,62]. Passive loading methods include the simple incubation of EXOs with drugs that diffuse into them along the concentration gradient [63]. Instead, the possible methods for the active encapsulation of selected cargo involve sonication, extrusion, or electroporation [64–66]. These methods temporally perturb the EXO lipid bilayer, allowing drugs to enter them.

These various approaches have different loading yields, which obviously depend on the properties of the cargo. The application of these methodologies in cardiovascular diseases is still in its infancy, but the results obtained treating other pathologies such as cancer generate great expectations.
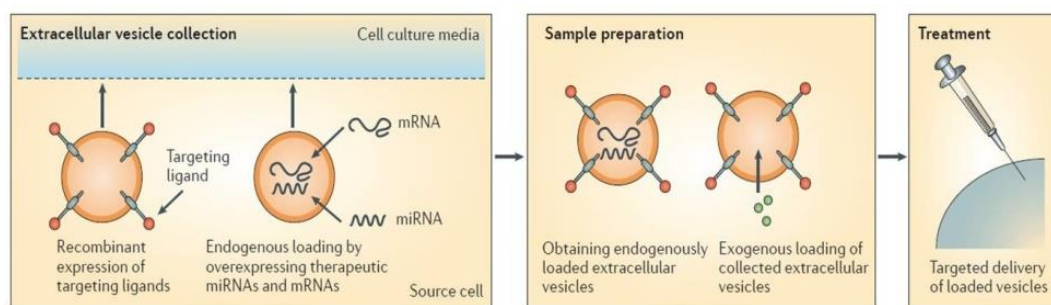

Figure 6. Engineering of extracellular vesicles (EVs). EVs can be engineered to load desired items, which can be carried out either endogenously or exogenously. Endogenous loading is achieved via transfecting parent cells strongly overexpressing miRNA or mRNA; this results in the production of EXOs that are already loaded with the elements of interest upon their collection. Exogenous loading allows the collection of drug-free EXOs which are then loaded with desired cargo molecules either via simple co-incubation with suitable cargo molecules or via active encapsulation with the help of certain procedures, such as electroporation. Modified from Reference [62].

5. Exosome Delivery to Target Cells

Despite the many advantages of the possibility of using EXOs as therapy in cardiovascular disease, a determining factor to make this possible is finding the right way to deliver them so they are effective.

For cardiovascular therapy, the ideal modality to deliver EXOs is obviously intravenous injection; however, it was demonstrated that this way predominantly led to absorption within the liver [67]. It was then tried to execute intramyocardial (IM) and intracoronary (IC) injections; the comparison between these two ways highlighted that EXO IM injection was more effective than IC injection [68]. Gallet and colleagues demonstrated that CDC EXO IM injections delivered in infarcted pig heart showed greater myocardial retention and, as a consequence, a significant decrease in scar size and in microvascular obstruction compared to IC delivery [68].

Vandergriff et al. highlighted that IM delivery in clinical practice is not the most eligible method because of its correlated risks [69]. To try solving the problem, they resorted to the modification of the EXO surface, a heavily researched area which aims to improve targeting of EXOs to cells of interest. In particular, they tried tagging EXOs with cardiac-homing peptide (CHP), a peptide that targets infarcted heart, and to inject them into the tail vein of infarcted rats [69]. This functionalization improved cardiac EXO retention, leading to the induction of CM proliferation, an increase in angiogenesis, and a reduction in heart fibrosis of infarcted rats [69]. In another study, Kim and colleagues generated EXOs that expressed cardiac-targeting peptide (CTP) bound to Lysosomal-associated membrane protein 2b (Lamp2b), an exosomal membrane protein, on the surface [70]. In vitro and in vivo experiments showed that CTP EXOs were preferentially delivered into heart cells and tissue, with an increase of 15% [71]. A peptide sequence, CSTSMLKAC, named ischemic myocardium-targeting peptide (IMTP), which targets ischemic areas of the heart, was discovered by Kanki et al. [71], and was utilized by Wang and colleagues to engineer the MSC EXO surface such that its cargo was released into injured CMs [72]. Their hypothesis was confirmed by in vivo experiments that highlighted a significant increase in targeting ischemic myocardium by IMTP-modified EXOs, leading to a significant improvement in cardiac health [72].

High retention in the liver is one of the biggest obstacles related to drug delivery, and EXOs addressed to the heart are not exempt from this problem. However, engineered EXOs seem to significantly improve the amount that reaches cardiac target cells.

6. Conclusions

The intent of this review was to take stock of the current state of the art regarding EXOs in cardiovascular diseases. This topic is of the great interest because the study of EXOs is revealing a lot of new information about paracrine cell communication, which is proving to be fundamental for the maintenance of physiologic organ homeostasis. Early studies immediately created great prospects for EXO use as therapy in many diseases, including cardiovascular ones. It soon became clear that they are advantageous compared to cell therapy, especially in this field, where whole-cell therapy seemed not promising [54]. Apart from their native properties, which can be exploited in therapy, they were shown to be suitable for modification so as to target drugs for specific cells and for use as biomarkers [17,46–51].

Study of the cardiac environment showed an amazing communication network, which exploits EXOs, between the various cardiac cells. This communication through EXOs was implied in the maintenance of cardiac homeostasis, but most of all in the adaptive response to stress signals. It follows that EXOs are involved in many cardiovascular process, having the capability to improve or worsen cardiac health [10–13]. For these reasons, many studies on EXO functions in cardiovascular disease continue to be carried out with the hope of exploiting them for developing new therapies for many cardiovascular pathologies.

In conclusion, this review highlighted that there is still a lot of work to be done before there are any real opportunities to use EXOs to treat cardiovascular diseases; standardized high-yield and non-expensive protocols to isolate and characterize EXOs remain to be developed. Furthermore, their

susceptibility to change makes it difficult to set up scalable and reproducible isolation processes. There are also no exhaustive studies about EXO kinetics, and many other points need to be deeply investigated. Instead, their use as biomarkers in the individualization of cardiac acute events might be a closer goal.

References

1. Simons, M.; Raposo, G. Exosomes—Vesicular carriers for intercellular communication. *Curr. Opin. Cell Biol.* **2009**, *21*, 575. [CrossRef] [PubMed]

2. Caradec, J.; Kharmate, G.; Hosseini-Beheshti, E.; Adomat, H.; Gleave, M.; Guns, E. Reproducibility and efficiency of serum-derived exosome extraction methods. *Clin. Biochem.* **2014**, *47*, 1286–1292. [CrossRef] [PubMed]

3. Ostrowski, M.; Carmo, N.B.; Krumeich, S.; Fanget, I.; Raposo, G.; Savina, A.; Moita, C.F.; Schauer, K.; Hume, A.N.; Freitas, R.P.; et al. Rab27a and Rab27b control different steps of the exosome secretion pathway. *Nat. Cell Biol.* **2010**, *12*, 19–30. [CrossRef] [PubMed]

4. Vizoso, F.J.; Eiro, N.; Cid, S.; Schneider, J.; Perez-Fernandez, R. Mesenchymal Stem Cell Secretome: Toward Cell-Free Therapeutic Strategies in Regenerative Medicine. *Int. J. Mol. Sci.* **2017**, *18*, 1852. [CrossRef] [PubMed]

5. Klumperman, J.; Raposo, G. The complex ultrastructure of the endolysosomal system. *Cold Spring Harb Perspect. Biol.* **2014**, *6*, a016857. [CrossRef] [PubMed]

6. Trajkovic, K.; Hsu, C.; Chiantia, S.; Rajendran, L.; Wenzel, D.; Wieland, F.; Schwille, P.; Brügger, B.; Simons, M. Ceramide triggers budding of exosome vesicles into multivesicular endosomes. *Science* **2008**, *319*, 1244–1247. [CrossRef] [PubMed]

7. Batagov, A.O.; Kuznetsov, V.A.; Kurochkin, I.V. Identification of nucleotide patterns enriched in secreted RNAs as putative cis-acting elements targeting them to exosome nano-vesicles. *BMC Genom.* **2011**, *12* (Suppl. 3), S18. [CrossRef]

8. Turturici, G.; Tinnirello, R.; Sconzo, G.; Geraci, F. Extracellular membrane vesicles as a mechanism of cell-to cell communication: Advantages and disadvantages. *Am. J. Physiol. Cell Physiol.* **2014**, *306*, 621–633. [CrossRef]

9. Dougherty, J.A.; Mergaye, M.; Kumar, N.; Chen, C.A.; Angelos, M.G.; Khan, M. Potential Role of Exosomes in Mending a Broken Heart: Nanoshuttles Propelling Future Clinical Therapeutics Forward. *Stem Cells Int.* **2017**, *2017*, 5785436. [CrossRef]

10. Malik, Z.A.; Kott, K.S.; Poe, A.J.; Kuo, T.; Chen, L.; Ferrara, K.W.; Knowlton, A.A. Cardiac myocyte exosomes: Stability, HSP60, and proteomics. *Am. J. Physiol. Heart Circ. Physiol.* **2013**, *304*, 954–965. [CrossRef]

11. Zhang, J.; Ma, J.; Long, K.; Qiu, W.; Wang, Y.; Hu, Z.; Liu, C.; Luo, Y.; Jiang, A.; Jin, L.; et al. Overexpression of Exosomal Cardioprotective miRNAs Mitigates Hypoxia-Induced H9c2 Cells Apoptosis. *Int. J. Mol. Sci.* **2017**, *18*, 711. [CrossRef] [PubMed]

12. Yu, X.; Deng, L.; Wang, D.; Li, N.; Chen, X.; Cheng, X.; Yuan, J.; Gao, X.; Liao, M.; Wang, M.; et al. Mechanism of TNF-α autocrine effects in hypoxic cardiomyocytes: Initiated by hypoxia inducible factor 1α, presented by exosomes. *J. Mol. Cell Cardiol.* **2012**, *53*, 848–857. [CrossRef] [PubMed]

13. Tian, C.; Gao, L.; Zimmerman, M.C.; Zucker, I.H. Myocardial infarction-induced microRNA-enriched exosomes contribute to cardiac Nrf2 dysregulation in chronic heart failure. *Am. J. Physiol. Heart Circ. Physiol.* **2018**, *314*, 928–939. [CrossRef] [PubMed]

14. Gupta, S.; Knowlton, A.A. HSP60 trafficking in adult cardiac myocytes: Role of the exosomal pathway. *Am. J. Physiol. Heart Circ. Physiol.* **2007**, *292*, 3052–3056. [CrossRef] [PubMed]

15. Waldenström, A.; Gennebäck, N.; Hellman, U.; Ronquist, G. Cardiomyocyte Microvesicles Contain DNA/RNA and Convey Biological Messages to Target Cells. *PLoS ONE* **2012**, *7*, e34653. [CrossRef] [PubMed]

16. Chaturvedi, P.; Kalani, A.; Medina, I.; Familtseva, A.; Tyagi, S.C. Cardiosome mediated regulation of MMP9 in diabetic heart: Role of mir29b and mir455 in exercise. *J. Cell Mol. Med.* **2015**, *19*, 2153–2161. [CrossRef] [PubMed]

17. Ha, D.; Yang, N.; Nadithe, V. Exosomes as therapeutic drug carriers and delivery vehicles across biological membranes: Current perspectives and future challenges. *Acta Pharm. Sin. B* **2016**, *6*, 287–296. [CrossRef] [PubMed]

18. Tang, Y.T.; Huang, Y.Y.; Zheng, L.; Qin, S.H.; Xu, X.P.; An, T.X.; Xu, Y.; Wu, Y.S.; Hu, X.M.; Ping, B.H.; et al. Comparison of isolation methods of exosomes and exosomal RNA from cell culture medium and serum. *Int. J. Mol. Med.* **2017**, *40*, 834–844. [CrossRef]

19. Laflamme, M.A.; Murry, C.E. Heart regeneration. *Nature* **2011**, *473*, 326–335. [CrossRef]

20. Barile, L.; Messina, E.; Giacomello, A.; Marban, E. Endogenous cardiac stem cells. *Prog. Cardiovasc. Dis.* **2007**, *50*, 31–48. [CrossRef]

21. Yang, Y.; Li, Y.; Chen, X.; Cheng, X.; Liao, Y.; Yu, X. Exosomal transfer of miR-30a between cardiomyocytes regulates autophagy after hypoxia. *J. Mol. Med.* **2016**, *94*, 711–724. [CrossRef] [PubMed]

22. Nie, X.; Fan, J.; Li, H.; Yin, Z.; Zhao, Y.; Dai, B.; Dong, N.; Chen, C.; Wang, D.W. miR-217 Promotes Cardiac Hypertrophy and Dysfunction by Targeting PTEN. *Mol. Ther. Nucleic Acids* **2018**, *12*, 254–266. [CrossRef] [PubMed]

23. Wang, X.; Huang, W.; Liu, G.; Cai, W.; Millard, R.W.; Wang, Y.; Chang, J.; Peng, T.; Fan, G.C. Cardiomyocytes mediate anti-angiogenesis in type 2 diabetic rats through the exosomal transfer of miR-320 into endothelial cells. *J. Mol. Cell Cardiol.* **2014**, *74*, 139–150. [CrossRef] [PubMed]

24. Garcia, N.A.; Ontoria-Oviedo, I.; González-King, H.; Diez-Juan, A.; Sepúlveda, P. Glucose Starvation in Cardiomyocytes Enhances Exosome Secretion and Promotes Angiogenesis in Endothelial Cells. *PLoS ONE* **2015**, *10*, e0138849. [CrossRef] [PubMed]

25. Cosme, J.; Guo, H.; Hadipour-Lakmehsari, S.; Emili, A.; Gramolini, A.O. Hypoxia-Induced Changes in the Fibroblast Secretome, Exosome, and Whole-Cell Proteome Using Cultured, Cardiac-Derived Cells Isolated from Neonatal Mice. *J. Proteome Res.* **2017**, *16*, 2836–2847. [CrossRef] [PubMed]

26. Bang, C.; Batkai, S.; Dangwal, S.; Gupta, S.K.; Foinquinos, A.; Holzmann, A.; Just, A.; Remke, J.; Zimmer, K.; Zeug, A.; et al. Cardiac fibroblast-derived microRNA passenger strand-enriched exosomes mediate cardiomyocyte hypertrophy. *J. Clin. Invest.* **2014**, *124*, 2136–2146. [CrossRef] [PubMed]

27. Lyu, L.; Wang, H.; Li, B.; Qin, Q.; Qi, L.; Nagarkatti, M.; Nagarkatti, P.; Janicki, J.S.; Wang, X.L.; Cui, T. A critical role of cardiac fibroblast-derived exosomes in activating renin angiotensin system in cardiomyocytes. *J. Mol. Cell Cardiol.* **2015**, *89*, 268–279. [CrossRef]

28. De Jong, O.; Verhaar, M.C.; Chen, Y.; Vader, P.; Gremmels, H.; Posthuma, G.; Schiffelers, R.M.; Gucek, M.; van Balkom, B.W.M. Cellular stress conditions are reflected in the protein and RNA content of endothelial cell derived Exosomes. *J. Extracell. Vesicles* **2012**, *1*, 18396. [CrossRef]

29. Sheldon, H.; Heikamp, E.; Turley, H.; Dragovic, R.; Thomas, P.; Oon, C.E.; Leek, R.; Edelmann, M.; Kessler, B.; Sainson, R.C.; et al. New mechanism for Notch signaling to endothelium at a distance by Delta-like 4 incorporation into exosomes. *Blood* **2010**, *116*, 2385–2394. [CrossRef]

30. Van Balkom, B.W.; de Jong, O.G.; Smits, M.; Brummelman, J.; den Ouden, K.; de Bree, P.M.; van Eijndhoven, M.A.; Pegtel, D.M.; Stoorvogel, W.; Würdinger, T.; et al. Endothelial cells require miR-214 to secrete exosomes that suppress senescence and induce angiogenesis in human and mouse endothelial cells. *Blood* **2013**, *121*, 3997–4006. [CrossRef]

31. Halkein, J.; Tabruyn, S.P.; Ricke-Hoch, M.; Haghikia, A.; Nguyen, N.Q.; Scherr, M.; Castermans, K.; Malvaux, L.; Lambert, V.; Thiry, M.; et al. MicroRNA-146a is a therapeutic target and biomarker for peripartum cardiomyopathy. *J. Clin. Invest.* **2013**, *123*, 2143–2154. [CrossRef] [PubMed]

32. Anversa, P.; Kajstura, J. Ventricular myocytes are not terminally differentiated in the adult mammalian heart. *Circ. Res.* **1998**, *83*, 1–14. [CrossRef]

33. Bergmann, O.; Bhardwaj, R.D.; Bernard, S.; Zdunek, S.; Barnabe-Heider, F.; Walsh, S.; Zupicich, J.; Alkass, K.; Buchholz, B.A.; Druid, H.; et al. Evidence for cardiomyocyte renewal in humans. *Science* **2009**, *324*, 98–102. [CrossRef] [PubMed]

34. Sahoo, S.; Klychko, E.; Thorne, T.; Misener, S.; Schultz, K.M.; Millay, M.; Ito, A.; Liu, T.; Kamide, C.; Agrawal, H.; et al. Exosomes from human CD34(+) stem cells mediate their proangiogenic paracrine activity. *Circ. Res.* **2011**, *109*, 724–728. [CrossRef] [PubMed]

35. Barile, L.; Gherghiceanu, M.; Popescu, L.M.; Moccetti, T.; Vassalli, G. Ultrastructural evidence of exosome secretion by progenitor cells in adult mouse myocardium and adult human cardiospheres. *J. Biomed. Biotechnol.* **2012**, *2012*, 354605. [CrossRef] [PubMed]

36. Barile, L.; Lionetti, V.; Cervio, E.; Matteucci, M.; Gherghiceanu, M.; Popescu, L.M.; Torre, T.; Siclari, F.; Moccetti, T.; Vassalli, G. Extracellular vesicles from human cardiac progenitor cells inhibit cardiomyocyte apoptosis and improve cardiac function after myocardial infarction. *Cardiovasc. Res.* **2014**, *103*, 530–541. [CrossRef] [PubMed]

37. Xiao, J.; Pan, Y.; Li, X.H.; Yang, X.Y.; Feng, Y.L.; Tan, H.H.; Jiang, L.; Feng, J.; Yu, X.Y. Cardiac progenitor cell-derived exosomes prevent cardiomyocytes apoptosis through exosomal miR-21 by targeting PDCD4. *Cell Death Dis.* **2016**, *7*, e2277. [CrossRef]

38. Barile, L.; Cervio, E.; Lionetti, V.; Milano, G.; Ciullo, A.; Biemmi, V.; Bolis, S.; Altomare, C.; Matteucci, M.; Di Silvestre, D.; et al. Cardioprotection by cardiac progenitor cell-secreted exosomes: Role of pregnancy-associated plasma protein-A. *Cardiovasc. Res.* **2018**, *114*, 992–1005. [CrossRef]

39. Ibrahim, A.G.E.; Cheng, K.; Marba'n, E. Exosomes as Critical Agents of Cardiac Regeneration Triggered by Cell Therapy. *Stem Cell Rep.* **2014**, *2*, 606–619. [CrossRef]

40. Huang, Y.; Crawford, M.; Higuita-Castro, N.; Nana-Sinkam, P.; Ghadiali, S.N. MiR-146a regulates mechanotransduction and pressure-induced inflammation in small airway epithelium. *FASEB J.* **2012**, *26*, 3351–3364. [CrossRef]

41. Wang, X.; Ha, T.; Liu, L.; Zou, J.; Zhang, X.; Kalbfleisc, J.; Gao, X.; Williams, D.; Li, C. Increased expression of microRNA- 146a decreases myocardial ischaemia/reperfusion injury. *Cardiovasc. Res.* **2013**, *97*, 432–442. [CrossRef] [PubMed]

42. Gray, W.D.; French, K.M.; Ghosh-Choudhary, S.; Maxwell, J.T.; Brown, M.E.; Platt, M.O.; Searles, C.D.; Davis, M.E. Identification of Therapeutic Covariant microRNA Clusters in Hypoxia Treated Cardiac Progenitor Cell Exosomes using Systems Biology. *Circ. Res.* **2015**, *116*, 255–263. [CrossRef] [PubMed]

43. Nie, S.; Wang, X.; Sivakumaran, P.; Chong, M.M.W.; Liu, X.; Karnezis, T.; Bandara, N.; Takov, K.; Nowell, C.J.; Wilcox, S.; et al. Biologically active constituents of the secretome of human W8B2+ cardiac stem cells. *Sci. Rep.* **2018**, *8*, 1579. [CrossRef] [PubMed]

44. Gallo, A.; Tandon, M.; Alevizos, I.; Illei, G.G. The majority of microRNAs detectable in serum and saliva is concentrated in exosomes. *PLoS ONE* **2012**, *7*, e30679. [CrossRef] [PubMed]

45. Kuwabara, Y.; Ono, K.; Horie, T.; Nishi, H.; Nagao, K.; Kinoshita, M.; Watanabe, S.; Baba, O.; Kojima, Y.; Shizuta, S.; et al. Increased microRNA-1 and microRNA-133a levels in serum of patients with cardiovascular disease indicate myocardial damage. *Circ. Cardiovasc. Genet.* **2011**, *4*, 446–454. [CrossRef]

46. Chan, D.; Ng, L.L. Biomarkers in acute myocardial infarction. *BMC Med.* **2010**, *8*, 34. [CrossRef] [PubMed]

47. Wang, G.K.; Zhu, J.Q.; Zhang, J.T.; Li, Q.; Li, Y.; He, J.; Qin, Y.W.; Jing, Q. Circulating microRNA: A novel potential biomarker for early diagnosis of acutemyocardial infarction in humans. *Eur. Heart J.* **2010**, *31*, 659–666. [CrossRef]

48. Li, Y.Q.; Zhang, M.F.; Wen, H.Y.; Hu, C.L.; Liu, R.; Wei, H.J.; Ai, C.M.; Wang, G.; Liao, X.X.; Li, X. Comparing the diagnostic values of circulating microRNAs and cardiac troponin T in patients with acute myocardial infarction. *Clinics (Sao Paulo)* **2013**, *68*, 75–80. [CrossRef]

49. Gidlöf, O.; Smith, J.G.; Miyazu, K.; Gilje, P.; Spencer, A.; Blomquist, S.; Erlinge, D. Circulating cardio-enriched microRNAs are associated with long-term prognosis following myocardial infarction. *BMC Cardiovasc. Disord.* **2013**, *13*, 12. [CrossRef]

50. Matsumoto, S.; Sakata, Y.; Suna, S.; Nakatani, D.; Usami, M.; Hara, M.; Kitamura, T.; Hamasaki, T.; Nanto, S.; Kawahara, Y.; et al. Circulating p53-responsive microRNAs are predictive indicators of heart failure after acute myocardial infarction. *Circ. Res.* **2013**, *113*, 322–326. [CrossRef]

51. Cheow, E.S.; Cheng, W.C.; Lee, C.N.; de Kleijn, D.; Sorokin, V.; Sze, S.K. Plasma-derived Extracellular Vesicles Contain Predictive Biomarkers and Potential Therapeutic Targets for Myocardial Ischemic (MI) Injury. *Mol. Cell Proteomics.* **2016**, *15*, 2628–2640. [CrossRef] [PubMed]

52. Chalmin, F.; Ladoire, S.; Mignot, G.; Vincent, J.; Bruchard, M.; Remy-Martin, J.P.; Boireau, W.; Rouleau, A.; Simon, B.; Lanneau, D.; et al. Membrane-associated Hsp72 from tumor-derived exosomes mediates STAT3-dependent immunosuppressive function of mouse and human myeloid-derived suppressor cells. *J. Clin. Investig.* **2010**, *120*, 457–471. [CrossRef]

53. Baietti, M.F.; Zhang, Z.; Mortier, E.; Melchior, A.; Degeest, G.; Geeraerts, A.; Ivarsson, Y.; Depoortere, F.; Coomans, C.; Vermeiren, E.; et al. Syndecan-syntenin-ALIX regulates the biogenesis of exosomes. *Nat. Cell Biol.* **2012**, *14*, 677–685. [CrossRef] [PubMed]

54. Cambria, E.; Pasqualini, F.S.; Wolint, P.; Günter, J.; Steiger, J.; Bopp, A.; Hoerstrup, S.P.; Emmert, M.J. Translational cardiac stem cell therapy: Advancing from first-generation to next-generation cell types. *NPJ Regen. Med.* **2017**, *2*, 17. [CrossRef] [PubMed]

55. Arslan, F.; Lai, R.C.; Smeets, M.B.; Akeroyd, L.; Choo, A.; Aguor, E.N.; Timmers, L.; van Rijen, H.V.; Doevendans, P.A.; Pasterkamp, G.; et al. Mesenchymal stem cell-derived exosomes increase ATP levels, decrease oxidative stress and activate PI3K/Akt pathway to enhance myocardial viability and prevent adverse remodeling after myocardial ischemia/reperfusion injury. *Stem Cell Res.* **2013**, *10*, 301–312. [CrossRef] [PubMed]

56. Feng, Y.; Huang, W.; Wani, M.; Yu, X.; Ashraf, M. Ischemic Preconditioning Potentiates the Protective Effect of Stem Cells through Secretion of Exosomes by Targeting Mecp2 via miR-22. *PLoS ONE* **2014**, *9*, e88685. [CrossRef]

57. Yu, B.; Kim, H.W.; Gong, M.; Wang, J.; Millard, R.W.; Wang, Y.; Ashraf, M.; Xu, M. Exosomes secreted from GATA-4 overexpressing mesenchymal stem cells serve as a reservoir of anti-apoptotic microRNAs for cardioprotection. *Int. J. Cardiol.* **2015**, *182*, 349–360. [CrossRef]

58. Zhang, Z.; Yang, J.; Yan, W.; Li, Y.; Shen, Z.; Asahara, T. Pretreatment of Cardiac Stem Cells With Exosomes Derived From Mesenchymal Stem Cells Enhances Myocardial Repair. *J. Am. Heart Assoc.* **2016**, *5*, e002856. [CrossRef]

59. Wang, Y.; Zhang, L.; Li, Y.; Chen, L.; Wang, X.; Guo, W.; Zhang, X.; Qin, G.; He, S.; Zimmerman, A.; et al. Exosomes/microvesicles from induced pluripotent stem cells deliver cardioprotective miRNAs and prevent cardiomyocyte apoptosis in the ischemic myocardium. *Int. J. Cardiol.* **2015**, *192*, 61–69. [CrossRef]

60. Middleton, R.C.; Rogers, R.G.; De Couto, G.; Tseliou, E.; Luther, K.; Holewinski, R.; Soetkamp, D.; Van Eyk, J.E.; Antes, T.J.; Marbán, E. Newt cells secrete extracellular vesicles with therapeutic bioactivity in mammalian cardiomyocytes. *J. Extracell. Vesicles* **2018**, *7*, 1456888. [CrossRef]

61. Zhang, Y.; Liu, D.; Chen, X.; Li, J.; Li, L.; Bian, Z.; Sun, F.; Lu, J.; Yin, Y.; Cai, X.; et al. Secreted monocytic miR-150 enhances targeted endothelial cell migration. *Mol. Cell* **2010**, *39*, 133–144. [CrossRef]

62. El Andaloussi, S.; Mäger, I.; Breakefield, X.O.; Wood, M.J. Extracellular vesicles: Biology and emerging therapeutic opportunities. *Nat. Rev. Drug Discov.* **2013**, *12*, 347–357. [CrossRef] [PubMed]

63. Sun, D.; Zhuang, X.; Xiang, X.; Liu, Y.; Zhang, S.; Liu, C.; Barnes, S.; Grizzle, W.; Miller, D.; Zhang, H.G. A novel nanoparticle drug delivery system: The anti-inflammatory activity of curcumin is enhanced when encapsulated in exosomes. *Mol. Ther.* **2010**, *18*, 1606–1614. [CrossRef] [PubMed]

64. Kim, M.S.; Haney, M.J.; Zhao, Y.; Mahajan, V.; Deygen, I.; Klyachko, N.L.; Inskoe, E.; Piroyan, A.; Sokolsky, M.; Okolie, O.; et al. Development of exosome-encapsulated paclitaxel to overcome MDR in cancer cells. *Nanomedicine* **2016**, *12*, 655–664. [CrossRef] [PubMed]

65. Fuhrmann, G.; Serio, A.; Mazo, M.; Nair, R.; Stevens, M.M. Active loading into extracellular vesicles significantly improves the cellular uptake and photodynamic effect of porphyrins. *J. Control. Release* **2015**, *205*, 35–44. [CrossRef]

66. Wahlgren, J.; De Karlson, T.; Brisslert, M.; Vaziri Sani, F.; Telemo, E.; Sunnerhagen, P.; Valadi, H. Plasma exosomes can deliver exogenous short interfering RNA to monocytes and lymphocytes. *Nucleic Acids Res.* **2012**, *40*, e130. [CrossRef]

67. Takahashi, Y.; Nishikawa, M.; Shinotsuka, H.; Matsui, Y.; Ohara, S.; Imai, T.; Takakura, Y. Visualization and in vivo tracking of the exosomes of murine melanoma B16-BL6 cells in mice after intravenous injection. *J. Biotechnol.* **2013**, *165*, 77–84. [CrossRef]

68. Gallet, R.; Dawkins, J.; Valle, J.; Simsolo, E.; de Couto, G.; Middleton, R.; Tseliou, E.; Luthringer, D.; Kreke, M.; Smith, R.R.; et al. Exosomes secreted by cardiosphere-derived cells reduce scarring, attenuate adverse remodelling, and improve function in acute and chronic porcine myocardial infarction. *Eur. Heart J.* **2017**, *38*, 201–211. [CrossRef]

69. Vandergriff, A.; Huang, K.; Shen, D.; Hu, S.; Hensley, M.T.; Caranasos, T.G.; Qian, L.; Cheng, K. Targeting regenerative exosomes to myocardial infarction using cardiac homing peptide. *Theranostics* **2018**, *8*, 1869–1878. [CrossRef]

70. Kim, H.; Yun, N.; Mun, D.; Kang, J.Y.; Lee, S.H.; Park, H.; Joung, B. Cardiac-specific delivery by cardiac tissue-targeting peptide-expressing exosomes. *Biochem. Biophys. Res. Commun.* **2018**, *499*, 803–808. [CrossRef]

71. Kanki, S.; Jaalouk, D.E.; Lee, S.; Yu, A.Y.; Gannon, J.; Lee, R.T. Identification of targeting peptides for ischemic myocardium by in vivo phage display. *J. Mol. Cell Cardiol.* **2011**, *50*, 841–848. [CrossRef] [PubMed]

72. Wang, X.; Chen, Y.; Zhao, Z.; Meng, Q.; Yu, Y.; Sun, J.; Yang, Z.; Chen, Y.; Li, J.; Ma, T.; et al. Engineered Exosomes with Ischemic Myocardium-Targeting Peptide for Targeted Therapy in Myocardial Infarction. *J. Am. Heart Assoc.* **2018**, *7*, e008737. [CrossRef] [PubMed]